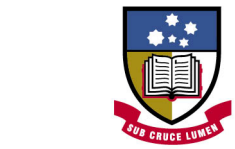

THE UNIVERSITY
of ADELAIDE

Many-Body Forces with Quark Meson Coupling

by

Nathanael Botten

In fulfilment of the requirements for the degree of

Master's of Philosophy

April 2024

School of Physics, Chemistry and Earth Sciences

Department of Physics

The University of Adelaide

Contents

List of Tables

List of Figures

Abstract

The quark-meson coupling (QMC) model is a phenomenological model which seeks to describe nuclear systems in terms of quark degrees of freedom. This is done by coupling the meson fields, which describe the nuclear force, to the valence quarks inside of the baryons. Considered in this work is a many-body expansion of the QMC model, extended to include strange baryons (hyperons). From here this expansion is applied to solve for the binding energy of a number of different situations.

The first of these applications is to fit the coupling constants in the model to the binding energies of Lambda hyperons. The binding energies for Lambda hyperons are known for several different nuclei, which makes it ideal for fitting the constants. This is completed by using previously established values for the coupling constants, and allowing for slight variations in the coupling constants, due to the many-body expansion being an approximation to the QMC model.

Following this, the coupling constants found will be used to predict the binding energies for a number of different cascade hyperons, which have 2-strange quarks instead. An isospin-dependent term is introduced here, which includes a new coupling constant, and so these are tested for a few different values of the coupling constant.

Next, a prediction for the effect of the nuclear potential on the binding of a negative cascade, bound by the Coulomb force into an iron atom, is made. This is done by calculating the energy levels of the 5g and 6h states to a high precision, and then finding the transition between them. This transition is compared to the case where there is no Coulomb potential, in order to investigate the effect the strong force has on the binding.

Finally, the mean contribution of the scalar meson field is calculated, for the binding of a Sigma hyperon in a helium nucleus. This value can then be used to make a prediction for the change in the magnetic moment between the Sigma hyperon in and out of the nuclear medium.

Declaration

I certify that this work contains no material which has been accepted for the award of any other degree or diploma in my name, in any university or other tertiary institution and, to the best of my knowledge and belief, contains no material previously published or written by another person, except where due reference has been made in the text. In addition, I certify that no part of this work will, in the future, be used in a submission in my name, for any other degree or diploma in any university or other tertiary institution without the prior approval of the University of Adelaide and where applicable, any partner institution responsible for the joint-award of this degree.

I acknowledge that copyright of published works contained within this thesis resides with the copyright holder(s) of those works.

I also give permission for the digital version of my thesis to be made available on the web, via the University's digital research repository, the Library Search and also through web search engines, unless permission has been granted by the University to restrict access for a period of time.

I acknowledge the support I have received for my research through the provision of an Australian Government Research Training Program Scholarship.

Nathanael Botten 21/4/2024

Acknowledgements

I would like to thank my supervisor Tony Thomas for his support throughout my Master's. I've had a really enjoyed working on this project, and it's in large part due to his guidance as I've sought to understand the QMC model, and also for his help in drafting this thesis. I'm also grateful to Jonathan Carroll, for providing me with his code for finding the energy eigenvalues in the Dirac equation. I'd also like to thank the other students from the CSSM and CDMPP departments. Particularly, Matthew Rumley, with whom I've enjoyed many conversations both on physics, philosophy, and life. I'd also grateful for the other members of the Fish Bowl, Cameron, James, Josh, Matthew, and Ted, for the joy of studying alongside them.

I'd also like to thank the members of the evangelical students club, for whom I'm grateful for friendship, and community while at university! Particularly I'd like to thank the other members of the 2022 executive committee, Bianca, Joel, Rachael, Steph, Jacob, and Reuben, who enabled me to serve as president while studying for this degree.

I'm also grateful to my parents, Rochelle and Jamie, who have taken an interest in my research, even though its not biology, and my sister, Bethany, who is a source of joy for my life.

Most of all, I'm grateful to my God, and saviour Jesus Christ, through whom I have been immeasurably blessed with the joy of studying his creation throughout this degree.

Introduction

Nuclear physics is the study of the interactions between baryons and the properties of such matter. This includes properties such as mass and binding energy, magnetic moments, and similar [1]. Inside the scope of nuclear physics is the study of finite nuclei, which are collections of protons and neutrons (together known as nucleons). Nuclear physics also extends to include the study of infinite nuclear matter. Infinite nuclear matter is matter where the number of nucleons present is taken towards infinity, which is in a naive sense, what is occurring in a neutron star [2].

In the past it was assumed that the appropriate degrees of freedom for doing nuclear physics were the nucleons. Indeed, the majority of nuclear properties can be described without an appeal to the nucleon structure [3]. However, if one ignores this structure, there still remains the question of the origin and exact nature of the nuclear force. Furthermore, at dense enough nuclear matter, such as that in neutron stars, it is postulated that quarks are the correct degrees of freedom for nuclear physics [2] [4]. Despite this, in nuclear physics, the current prevailing opinion remains that the nuclear physicist can ignore nucleon structure, at least in the majority of cases, due to the energy scale of nuclear physics [5].

In order to investigate nuclear phenomena then, a popular approach is to consider an effective field theory. These are quantum field theory approaches, which include the degrees of freedom to be investigated, be that the nucleon or quark, along with all the appropriate symmetries. One such approach in the field, which has accomplished this, is a theory known as quantum hadrodynamics (QHD). In QHD the hadrons are considered the correct degrees of freedom, coupled to a number of different meson fields [6] [7]. Then, in this model, one could consider the nuclear force as the result of virtual mesons being exchanged between the hadrons.

However, should one still remain curious as to whether or not this structure is indeed irrelevant to the interactions in nuclear matter, one might consider a couple of different options to proceed. One possible option would be to consider using quantum chromodynamics (QCD) to describe the nuclear environment. But as shall soon be seen, due to the complexity of this theory, it is not really possible to apply QCD to a full nuclear environment.

Due to these restraints, for the time being, the best alternative option is to turn to a

phenomenological model, where the quarks are the degrees of freedom, to describe the nuclear environment. One such phenomenological model is the Quark-Meson Coupling (QMC) model [4]. This model shares some similarities to QHD. The key difference is that instead of coupling the meson fields to the nucleons, the QMC model couples the meson fields to the quarks inside of the nucleons, and hence the nucleons are not structureless in this model.

In past work, a many-body expansion of the QMC Hamiltonian has been found for nucleons [8]. This allowed for the comparison of the QMC model to the Skyrme effective force, which upon fitting the coupling constants in the model, led to a good degree of agreement between these two descriptions [9] [10]. This provides some amount of confidence that making use of this type of many-body expansion is a legitimate endeavour. It is then of interest to see how this expansion might extend to strange quark nuclear material.

To this end, this work intends to investigate the binding of strange quark baryons, or hyperons, into finite nuclear matter. There has already been quite a bit of work done investigating the binding of Lambda hyperons, where a number of experiments have been carried out to establish the binding energy for a number of different hypernuclei [11]. There have also been past attempts to find a phenomenological model which accounts for these binding energies [12] [13]. Despite a relative abundance of investigation into one strange quark nuclear material, there is still quite a bit unknown about scenarios where two strange quarks are present [14]. This makes it of interest to investigate how this expansion of the QMC model might fare in these cases. The QMC model has also in past been used to investigate strange quark nuclear systems [15] [16] [17]. Where this work shall differ from this past work is by implementing a simple many-body approximation, and carrying out the calculations of the binding energies using more recent calculations of the coupling constants for the quarks to the meson fields.

This thesis will begin with a brief overview of background concepts pertinent to the QMC model in ch. [1]. Following this, in ch. [2], the QMC model will be introduced, beginning with a derivation of how to find the classical energy of a nucleon in the QMC model, and then using the classical energy, the Hamiltonian will be expanded in terms of the many-body forces.

With the background needed to understand the model established, in ch. [3] the many-body expansion will be extended to Λ^0 hyperons, in which there is one strange quark, and the remaining quarks have zero isospin. With the expansion established we will then be in a position to calculate the binding energies of the Λ hyperons. The binding energies will be calculated from the Schrödinger equation, which can be solved using a Numerov algorithm. The Λ binding energies in finite nuclear matter are relatively well established so from these a best fit for the coupling constants in the

QMC model will be found.

Using the coupling constants determined from the Λ binding, in ch. [4] the binding energies of both the Ξ^0 and Ξ^- cascade hyperons will be investigated. These will now include both an isospin dependent contribution, and for the Ξ^- a Coulomb interaction is also included. The derivation for both of these terms will be included in this chapter. Following this the splitting in the atomic energy levels due to the nuclear interaction will be investigated in ch. [5]. This will be carried out in an iron nucleus, and compared to the analytical solution for a point-like iron nucleus. Iron has been chosen first, as an experiment has already been carried out on iron targets [18]. Following this, Carbon has also been proposed as a target, and so similar calculations will be carried out for a carbon nucleus [19].

Finally, a brief investigation of some of the properties of nuclear matter in the case of the binding of Σ^0 hyperon will be carried out, in ch. 6]. This will include the calculation of the mean σ meson field in ^{4}He, as thus far the Σ^0 has only been found to be bound into a Helium nucleus [20] [21].

Chapter 1

Background Information

To begin, we shall first consider a number of important concepts that are needed to understand the QMC model. This will include a brief overview of the particle physics and QCD concepts relevant to the model. Following this a number of different types of hadrons, relevant to this project, will be introduced. With this, the MIT bag model will then be introduced. The MIT bag model is a model for hadron structure, which aims to capture the key features of QCD, namely confinement of the quarks. Finally, a brief discussion on nuclear physics will be had, where some of the usual practices in the field, and key concepts will be introduced.

1.1 Particle Physics Background

Currently, the prevailing model for matter is that it is made up of particles, as postulated in the standard model [22]. One of the striking features about these particles is that particles of a given variety are indistinguishable. That is to say that should one observe an electron, then they would know what all electrons are like.

The understanding of particles has evolved quite a bit over time, however the current way they are understood is formulated in a quantum field theory. In quantum field theory particles are thought of as excitations in a quantum field [22] [23]. This leads to a natural understanding of how particles interact with each other over a distance. These interactions are considered to be mediated by the fields, which in turn leads to understanding these interactions as the exchange of virtual particles.

The standard model has been demonstrated to describe three of the four elementary forces, with this interpretation. The particles which mediate these forces are known as gauge bosons. These gauge bosons are the photon for the electromagnetic force, the W and Z bosons for the weak force, and the gluon for the strong force.

In addition to these particles, the standard model also includes the description of quarks, leptons and the Higgs boson. Particularly relevant to this work are quarks,

as quarks are the fundamental particles which form baryons. The quark model arose from the work of Gell-Mann and Zweig [24], independently. Gell-Mann had already introduced the idea of the 'eight-fold way' [25], which organised the known baryons and mesons by their charge and strangeness, but left open the question as to why they could be arranged this way.

1.2 QCD Background

This question was eventually explained through the postulation of quarks, and gluons [26] [27]. This led to the development of a quantum field theory, QCD, which describes the interactions between quarks and gluons. Quarks and gluons carry a property known as colour. Colour follows an SU(3) gauge theory, with the option of quarks being red, green or blue [28]. In addition, quarks also carry another quantum number known as flavour. There are six options for quark flavours, up, down, strange, charm, top, or bottom. Of particular relevance to this work are the up, down and strange quarks. Now we note, that SU(3) is a non-Abelian gauge symmetry group, and thus the generators of the theory do not commute. Thus, the QCD Lagrangian can be expressed as below, neglecting the flavour arguments here for brevity [23]:

$$\mathcal{L} = \bar{\psi}(i\not{\partial} - m)\psi - \frac{1}{4}(\partial_\mu A^a_\nu - \partial^a_\nu)^2 + gA^a_\mu \bar{\psi}\gamma^\mu t^a \psi \\ - gf^{abc}(\partial_\mu A^a_\nu)A^{\mu b}A^{\nu C} - \frac{1}{4}g^2(f^{eab}A^a_\mu A^b_\nu)(f^{ecd}A^{\mu c}A^{\nu d}) \quad (1.1)$$

Where here, ψ is the quark wavefunction, A^a_μ are the gluon fields, g is the coupling constant for the theory, f^{abc} are the structure constants, and t^a is a matrix representation of the underlying Lie algebra of the generators.

From this Lagrangian we can deduce the types of interactions between the quarks and gluons. Namely, we can see from the third term, that there is a gluon-quark interaction vertex, from the fourth term a three gluon vertex, and from the fifth term a four gluon vertex. The gluon self-interaction vertices differentiate QCD from QED, as in QED the photon cannot interact with itself. It is these self-interaction vertices which lead to a peculiar QCD phenomena, known as confinement. Confinement ultimately results in all physical hadrons being in colour singlet, or colour neutral, states. This leads to a prediction that there are no isolated quarks or anti-quarks, but only ever quarks or anti-quarks confined into hadrons. Instead, should one try to separate out a quark the gluon field would form what is called a 'flux tube.'The energy required to separate this quark from the gluon field grows linearly with distance, which leads to the confinement of the quarks [29]. This all leads to a picture of the nucleon as a complicated environment!

Now, due to the complexity introduced by the self-interaction of the gluon fields, QCD currently has no analytical solution. The primary way that QCD is explored is through a computational scheme, known as lattice QCD. Unfortunately lattice QCD is rather computationally expensive, for even simple systems. A full nuclear environment is from a QCD perspective, an incredibly complex system, and as the number of nucleons present increases, this problem is made far more complicated by the increasing complexity of the possible interactions [30]. So, if we are interested in finding how the quark structure effects nuclear physics properties, what possible means are available to us?

1.2.1 From QCD to Nuclear Physics

Well, despite the challenge of increased complexity in the nuclear environment, there have been some attempts at applying lattice QCD to calculate nuclear physics properties. These have included both investigations into finding the nucleon-hyperon potential [31], and also to investigating properties like the magnetic moments of nuclei [32]. However, these attempts are not considering large nuclei, which remain an impractical way to attempt to solve the problem.

If QCD is not a viable way to investigate how nucleon structure effects nuclear properties, then an alternative way to approach the problem would be to consider an effective field theory. On this view then, the nuclear force is considered to be a residual effect, caused by the 'leaking' of the strong force outside of the baryons [5]. The underlying principle in effective field theories is that there is some amount of independence for the physics which occurs at a given energy scale, from the physics that happens at another energy scale. This is to say that a given effective field theory consists with the particles of interest, as the degrees of freedom, alongside all the symmetries of the system, without considering what might be happening at other energy scales [33]. In general, this is not an unreasonable principle for doing physics; one does not need quantum mechanics to describe the motion of the solar system. But the question then remains what are the appropriate degrees of freedom? It is thus a central premise for the QMC model that the quarks are the correct degree of freedom, and not the nucleons.

1.3 Baryons and Mesons in the QMC Model

Throughout this work a number of different baryons and mesons will be explored. The QMC model describes the nuclear environment by coupling these different meson fields to the quarks inside of the baryons. And so to accurately describe the forces in the nuclear environment we will include different mesons to mediate certain aspects of the force. Let us first consider the different baryons to be considered in this work, before

Baryon	Quark Content	Electric Charge [q_e]	I_z	Strangeness	Mass [MeV]
Proton	uud	+1	$+\frac{1}{2}$	0	938.272
Neutron	udd	0	$-\frac{1}{1}$	0	939.565

Table 1.1: Table Summarising relevant Nucleon quantum numbers

Hyperon	Quark Content	Electric Charge [q_e]	I	I_z	Strangeness	Mass [MeV]
Λ^0	uds	0	0	0	-1	1115.683
Σ^0	uds	0	1	0	-1	1192.642
Ξ^0	uss	0	$\frac{1}{2}$	$+\frac{1}{2}$	-2	1314.86
Ξ^-	dss	-1	$\frac{1}{2}$	$-\frac{1}{2}$	-2	1321.71
Ω^-	sss	-1	0	0	-3	1672.45

Table 1.2: Table Summarising relevant Hyperon quantum numbers

turning to the mesons describing the different interactions.

1.3.1 Baryons

The simplest, and most common types of baryons dealt with in this work are the protons and neutrons, collectively called nucleons. These can be grouped together to create objects called nuclei. Nuclei are classified by both their nucleon number, which is the total number of nucleons present, and the proton number, which is the number of protons present. The properties of the nucleons are summarised in table [1.1].

The other type of baryons considered will be those containing strange quarks, which are also called hyperons. When a hyperon is present in a nucleus, it is called a hypernuclei. The properties of the different types of hyperons considered here, are found in table [1.2].

Here we have already been introduced to a number of important properties considered throughout this work. The first of which is isospin, denoted as I. Isospin is a property which up and down quarks each possess. Up and down quarks both have an isospin of a half [28]. It is possible as well for the isospin of these quarks to be aligned or anti-aligned, which is what distinguishes the Λ^0 and the Σ^0, as can be seen in table [1.2]. However, isospin has different components. The most important component of the isospin is the third component, I_z or sometimes I_3. For this component of the isospin, the up and down quarks differ, where the up quark has $I_z = +\frac{1}{2}$ and the down quark has $I_z = -\frac{1}{2}$. So, although the Λ^0 and Σ^0 have differing values of isospin, they each have a third component of isospin of zero.

The other important quantum number to define is the strangeness. The strangeness is defined as the number of anti-strange quarks, subtract the number of strange quarks,

$S = n_{\bar{s}} - n_s$. Thus, we see that the strangeness is negative for each of the hyperons we investigate here [22]. Strangeness is a conserved quantity in strong interactions [28], which is important for this work, as throughout we shall not account for interactions where the strange quarks decay to up and down quarks. The meson fields which mediate the forces in this work are considered as the leaking of the strong force, and these interactions should not cause the strangeness of the hyperons to change.

1.3.2 Mesons

In this work, there are three mesons considered to be mediating the nuclear force. Importantly, the mesons considered here are all composed of only up and down quarks, and their anti-particles.So, as these mesons do not have any strange quarks, a simple approximation, motivated by the Okubo-Zweig-Iizuka rule (OZI rule) [22], will be that the strange quarks will not couple to the meson fields. This rule states that QCD processes where the Feynmann diagram can be disconnected into two separate diagrams by imagining a 'cut' across only gluon lines will be suppressed [34]. Hence, the meson field interactions with the strange quarks in the hyperons are suppressed, compared to those with the up and down quarks in the hyperons. This results in an overall reduction in the coupling of the meson fields to a Lambda hyperon compared to that of a nucleon.

σ Meson

The σ meson is a scalar isoscalar meson. This means that it has a net spin of zero, as the constituent quarks have anti-aligned spins. It also has zero isospin. Here then, the sigma meson will couple equally to the up and down quarks in a baryon. The Lagrangian density which describes the coupling of the scalar meson to these quarks is given by:

$$\mathcal{L}_{\sigma\ Int} = g_\sigma^q \bar{q} \sigma q \tag{1.2}$$

As can be seen from the interaction term here, the interaction with the sigma field acts similarly to the mass term in the Dirac equation. In this way, the interaction with the sigma field can be understood as adjusting the quark mass. However, this process then introduces an ambiguity in the exact mass of the σ meson, in the nuclear medium. It is thus often treated as a parameter in any fit being done, with values taken to be around $m_\sigma = 500$MeV [8] [35].

ω Meson

The ω meson is a vector isoscalar meson. So here, the quark and antiquark pair have aligned spins. However, this meson still has an isospin of zero. So, the ω meson inter-

action with both up and down quarks is the same. The Lagrangian density describing the coupling of the ω meson to these quarks is given by:

$$\mathcal{L}_{\omega\ Int} = g^q_\omega \bar{q}\gamma^\mu \omega_\mu q \tag{1.3}$$

The mass for the ω meson is given by $m_\omega = 783$MeV [8]. Furthermore, each of the components of the ω field each satisfy the Klein-Gordon equation individually.

ρ Meson

The final meson considered in this work is the ρ meson, which is both a vector and isovector meson. So similarly, to the ω meson, the ρ has quarks with aligned spin. However, as the isospin is non-zero for this meson it will couple differently to the up and down quarks inside the baryons in the QMC model. The Lagrangian density describing the interaction of the ρ and a quark is given by:

$$\mathcal{L}_{\rho\ Int} = g^q_\rho \bar{q}\gamma^\mu \frac{\tau^\alpha}{2} \rho^\alpha_\mu q \tag{1.4}$$

Here τ represents the Pauli matrices, which introduce the dependence on the isospin of the quarks. The mass of the ρ is given by $m_\rho = 770$ [8].

1.4 Baryon Structure

It is known that nucleons are not point particles, but rather have an underlying structure. And it is one of the central premises of this thesis that this underlying structure has some effect on nuclear physics. And thus, in order to properly carry out this work, there is a need to have a model for the baryon structure.

In order to capture this structure, it is important that the model for nucleon structure exhibits confinement. There are a number of different models which try to describe this. The type of model focused on here will be a class of models known as bag models. These are simple models where the quarks are restricted to be inside an area of space called a bag. Particularly, throughout this work the MIT bag model will be employed.

1.4.1 MIT Bag Model

The MIT bag model is a model initially proposed by Chodos et al. [36] [37]. This model describes the nucleon as three valence quarks, constrained within a spherical bag. The final element to this model is that there is a constant amount of energy required to produce and sustain this bag. The Lagrangian density then for this model, inside the bag, is simply given by:

$$\mathcal{L}_{MIT} = \bar{q}(i\gamma^{\mu}\partial_{\mu} - m_q)q - BV \tag{1.5}$$

The first term here is a Dirac equation for the quark fields, with the mass term being that for the mass of a quark, m_q. Here B, is the energy density, which takes a constant value. The effect of adding this term amounts to picking up an extra term in the energy-momentum tensor, such that you find: $T^{\mu\nu} = T^{\mu\nu}_{\text{Fields}} - Bg^{\mu\nu}$, while inside the bag, and when outside the bag the energy-momentum tensor vanishes. This implies that the quarks inside are confined, as we desire for our model of nucleon structure. The boundary condition on the surface of the bag, where $r = R$, amounts to:

$$(1 + i\vec{\gamma} \cdot \hat{r})q = 0 \tag{1.6}$$

1.5 Nuclear Physics Background

With the needed background for both the particle physics, and baryon structure dealt with, we shall now turn to considering how nuclear forces are commonly described, in terms of many-body forces. Then we shall briefly survey an alternative description of nuclear physics, QHD.

1.5.1 Many-Body Forces in Nuclear Physics

The first microscopic description of the nuclear force was given by Yukawa, which was described by an exchange of virtual pions [5]. These exchanges can lead to interactions between 2 or 3 nucleons. These are known as many-body forces, based on the number of nucleons involved.

However with the discovery of many more types of heavier mesons, it has become apparent that this simple model of the nuclear force would be inadequate [22]. Now there could be much more complex interactions, involving the exchange of not only pions, but also of the other mesons, such as the σ, ω, ρ or even other heavier strange quark mesons. This is to be expected, as knowing that nucleons are actually intricate objects with many moving parts, one might expect to find a more complex description of their forces. Despite there being now more possible options for the meson exchanged between nucleons, the fundamental idea of many-body forces remains applicable. Even more interesting is to note that not all types of mesons contribute to higher-order many-body forces, as will be seen for the vector mesons in this work.

1.5.2 Quantum Hadrodynamics

Due to the complexity of baryon structure, and the challenges it produces, a sensible place to begin to investigate the nuclear force would be through an effective field theory.

One of these effective field theories which shares some similarities with the QMC model is quantum hadrodynamics (QHD). This model couples the meson fields introduced in section [1.3.2], to the nucleons, treated as structureless Dirac particles [6].

In this way, the model circumvents the problem of the underlying quark structure. It is noted that this will lead to increasing complexity at short distance, due to the break down of the hadronic description [7]. With this being said, the QHD model does include both explicit dependence on the meson fields, due to the couplings, in a relativistic way, which are desirable properties for a theory of the nuclear force.

1.5.3 Binding Energy

Finally, we shall consider what is the primary property calculated throughout this work, the binding energy. The binding energy is defined as the energy that it takes to remove a baryon from a nucleus. This is the difference between the energy of the baryon when bound in the nucleus, compared to when it is free.

$$E_{Binding} = E_{Bound} - E_{Free} \tag{1.7}$$

The energy of a free state is larger than that of a nucleon in a bound system, and thus binding energy is negative, as one might expect for a bound state. Throughout this project, we shall find the binding energy by finding the ground state energy of a baryon, bound into the nuclear environment described by a many-body potential.

In nuclear physics it is also common to consider the average binding energy per nucleon, for a nucleus. For small nuclei this is found to increase rapidly with nuclear size, however, at a certain nuclear size the binding energy per nucleon begins to remain relatively constant [3]. This is a process which is known as saturation. Saturation is caused by nucleons only interacting with the other neighbouring nucleons [38]. In larger nuclei, the number of nucleons interacting with the maximum number of neighbours is larger than in smaller nuclei, which leads to the average binding energy per nucleon to remain roughly constant for larger nuclei. This once again changes however for very large nuclei, as the Coulomb force begins to have a greater impact on the binding energy, leading to a reduction in the binding energy per nucleon [39].

Chapter 2

Introducing the QMC Model

2.1 Setting up the QMC Model

The QMC model functions by coupling the meson fields to the valence quarks inside of the baryons of interest. This provides a method to investigate how the underlying baryon structure contributes to nuclear effects. As we saw in section [1.4.1], the MIT bag model makes for a simple model with which we can describe the nucleon structure. From here, we will consider a derivation of the classical energy for a nucleon in the nuclear environment, in the QMC model, following closely from the work of Guichon et al. [4].

We begin by considering the coordinates, of a nucleon, in the rest frame of the nucleus (NRF henceforth). These are denoted as $(t, \vec{r})$ throughout. Then the nucleon can be described following a classical trajectory through the nuclear environment, given by $\vec{R}(t)$, with a corresponding velocity:

$$\vec{v} = \frac{d\vec{R}}{dt} \tag{2.1}$$

And thus, the instantaneous rest frame (IRF henceforth), can be defined for the nucleon, with coordinates $(t', \vec{r'})$. Then, the transformation between these two systems is given by:

$$r_{||} = r'_{||} \cosh\eta + t' \sinh\eta \tag{2.2}$$

$$r_{\perp} = r'_{\perp} \tag{2.3}$$

$$t = t' \cosh\eta + r'_{||} \sinh\eta \tag{2.4}$$

Where we have the rapidity $\tanh\eta = |\vec{v}(t)|$, $r_{||}$ are the components parallel to the velocity, and $r_{\perp}$ are the components transverse to the velocity.

The benefit of defining the coordinates in this way is that in the IRF, it is reasonable to implement the MIT bag model, introduced in [1.4.1]. Thus we have a solution for the quark fields in the IRF. From here, it is necessary to couple the quark fields to the meson fields. In the NRF we expect that the meson fields are simply functions of position, generated by the nuclear environment. Hence they are given by $\sigma(\vec{r})$, $\omega^{\mu}(\vec{r})$, and $\rho^{\mu}_{\alpha}(\vec{r})$. We note that the ρ meson can be treated in a similar manner to the ω meson due to both being vector mesons. So from here we shall neglect the ρ meson, until we reintroduce it by analogy in equation [2.41].

Now we simply need to transform these meson fields to the IRF. We denote the coordinate for the position of the quark from the center of a bag, $\vec{u}' = \vec{r}' - \vec{R}'$. Then this follows a simple Lorentz transformation, such that:

$$\sigma'(t', \vec{u'}) = \sigma(\vec{r}) \tag{2.5}$$
$$\omega'^{0}(t', \vec{u'}) = \omega(\vec{r}) \cosh\eta \tag{2.6}$$
$$\omega'^{i=1,2,3}(t', \vec{u'}) = -\omega(\vec{r})\hat{v} \sinh\eta \tag{2.7}$$

And hence we can couple the quarks to the mesons, resulting in the interaction Lagrangian in the IRF:

$$\mathcal{L}_I = g^q_{\sigma}\bar{q'}q'(u')\sigma'(u') - g^q_{\omega}\bar{q'}\gamma_{\mu}q'(u')\omega'^{\mu}(u') \tag{2.8}$$

From here we aim to find the Hamiltonian in the IRF. To do this we begin by considering the nucleon position $\vec{R}$ at time T in the NRF, and consider the transformation:

$$R_{||} = R'_{||}\cosh\eta + t' \sinh\eta \tag{2.9}$$
$$R_{\perp} = R'_{\perp} \tag{2.10}$$
$$T = t' \cosh\eta + R'_{||} \sinh\eta \tag{2.11}$$

Then for a point in the bag, $\vec{r}' = \vec{u}' + \vec{R}'$, at the same time t', we had the relation as in eqn. [2.2]. Thus we can conclude that:

$$r_{||} = R'_{||}\cosh\eta + t' \sinh\eta + u'_{||}\cosh\eta \tag{2.12}$$
$$= R_{||} + u'_{||}\cosh\eta \tag{2.13}$$
$$\vec{r}_{\perp} = \vec{R}_{\perp} + \vec{u}'_{\perp} \tag{2.14}$$

And substituting these coordinate transforms into the σ field:

$$\sigma_{IRF}(u') = \sigma(R_{||}(T) + u'_{||}\cosh\eta, \vec{R}_{\perp}(T) + \vec{u}'_{\perp}) \tag{2.15}$$

And for the ω field, we find:

$$\omega_{IRF}(u')'^{0} = \omega(R_{||}(T) + u'_{||}\cosh\eta)\cosh\eta \tag{2.16}$$

$$\omega_{IRF}^{i=1,2,3}(u')' = -\omega(\vec{u'}_{\perp} + \vec{R}_{\perp}(T))\hat{v}\sinh\eta \tag{2.17}$$

With this we can apply the Born-Oppenheimer approximation, which allows us to solve for the equations of motion of the quarks, while we take $\vec{R}(T)$ as a fixed parameter. That is to say we shall take:

$$\sigma_{IRF}(t', \vec{u'}) \approx \sigma(\vec{R}(T)) \tag{2.18}$$

2.2 QMC Lagrangian & Classical Nucleon Energy

With the form for the meson fields in the IRF established, it is now possible to write a Lagrangian for the QMC model.

$$\mathcal{L}_{Int} = g_\sigma^q \bar{q'} q'(t', \vec{u'})\sigma(\vec{R} + \vec{u'}) - g_\omega^q \bar{q'}\left[\gamma^0\cosh\eta + \vec{\gamma}\cdot\hat{v}\sinh\eta\right] q'(t', \vec{u'})\omega(\vec{R} + \vec{u'}) \tag{2.19}$$

Then the Hamiltonian would be given by:

$$\begin{aligned} H = BV + \int_0^{R_B} d\vec{u'}\bar{q'}[&-i\vec{\gamma}\cdot\vec{\nabla} + m_q \\ &- g_\sigma^q\sigma(\vec{R} + \vec{u'}) + \left[\gamma^0\cosh\eta + \vec{\gamma}\cdot\hat{v}\sinh\eta\right]\omega(\vec{R} + \vec{u'})]q'(t', \vec{u'}) \end{aligned} \tag{2.20}$$

Then this can be split into a Hamiltonian in two parts:

$$H = H_0 + H_1 \tag{2.21}$$

Where these are given by:

$$\begin{aligned} H_0 = BV + \int_0^{R_B} d\vec{u'}\bar{q'}[&-i\vec{\gamma}\cdot\vec{\nabla} + m_q - g_\sigma^q\sigma(\vec{R}) \\ &+ g_\omega^q\bar{q'}\left[\gamma^0\cosh\eta + \vec{\gamma}\cdot\hat{v}\sinh\eta\right]\omega(\vec{R} + \vec{u'})]q'(t', \vec{u'}) \end{aligned} \tag{2.22}$$

$$\begin{aligned} H_1 = \int_0^{R_B} d\vec{u'}\bar{q'}[&-g_\sigma^q(\sigma(\vec{R} + \vec{u'}) - \sigma(\vec{R})) \\ &+ g_\omega^q(\omega(\vec{R} + \vec{u'}) - \omega(\vec{R}))(\gamma^0\cosh\eta + \vec{\gamma}\cdot\hat{v}\sinh\eta)]q'(t', \vec{u'}) \end{aligned} \tag{2.23}$$

At this point, we note that H_1 acts as a perturbation, but we shall ignore it in this work. This term turns out to correspond to a spin-orbit term which is known to be a very small term for Λ hyperons [40], and thus is negligible in the applications considered here.

With this noted, we continue, by first considering a set of eigenfunctions, ϕ^α which are complete and orthogonal, defined by:

$$h\phi^\alpha(\vec{u'}) = (-i\gamma^0\vec{\gamma}\cdot\vec{\nabla} + m_q^*\gamma^0)\phi^\alpha(\vec{u}') \tag{2.24}$$

$$= \frac{\Omega_\alpha}{R_B}\phi^\alpha(\vec{u}') \tag{2.25}$$

Which we take to have eigenvalues Ω_α/R_B, where Ω_α are the eigenfrequencies, corresponding to quantum numbers with the label α, and R_B is the bag radius. Here, m_q^* is not the physical quark mass. For now, we note that m_q^* will be the quark mass, plus the local scalar attraction. The solution to the lowest energy positive mode is known, and given by:

$$\phi^{0m}(t', \vec{u}') = \mathcal{N}\begin{pmatrix} j_0(\frac{xu'}{R_B}) \\ i\beta_q\vec{\sigma}\cdot\hat{u}' j_1(\frac{xu'}{R_B}) \end{pmatrix}\frac{\chi_m}{\sqrt{4\pi}} \tag{2.26}$$

With:

$$\Omega_0 = \sqrt{x^2 + (m_q^* R_B)^2} \tag{2.27}$$

$$\beta_q = \sqrt{\frac{\Omega_0 - m_q^* R_B}{\Omega_0 + m_q^* R_B}} \tag{2.28}$$

$$\mathcal{N} = x/\left\{ j_0(x)\sqrt{2R_B^3\left[\Omega_0(\Omega_0 - 1) + m_q^* R_B/2\right]}\right\} \tag{2.29}$$

Then the quark field will be given by an expansion of the different energy modes:

$$q'(t', \vec{u}') = \sum_\alpha e^{-i\vec{k}\cdot\vec{u}'}\phi^\alpha(\vec{u}')b_\alpha(t') \tag{2.30}$$

Where b_α is a annihilation operator for the given mode. And here $\vec{k}$ is chosen such that:

$$\vec{k} = g_\omega^q\omega(\vec{R})\hat{v}\sinh\eta \tag{2.31}$$

Then substituting the quark fields into H_0:

$$H_0 = \sum_\alpha \frac{\Omega_\alpha}{R_B} b_\alpha^\dagger b_\alpha - \sum_{\alpha\beta} \left\langle \alpha \left| (g_\sigma^q \sigma(\vec{R}) - m_q + m_q^*)\gamma^0 \right| \beta \right\rangle b_\alpha^\dagger b_\beta + \hat{N}_q g_\omega^q \omega(\vec{R}) \cosh\eta + BV \tag{2.32}$$

Then by choosing $m_q^* = m_q - g_\sigma^q \sigma(\vec{R})$, the matrix elements which involve the mixing of states $|\alpha\rangle$ and $|\beta\rangle$ for $\alpha \neq \beta$ are eliminated, thus reducing the problem to:

$$H_0 = \sum_\alpha \frac{\Omega_\alpha(\vec{R})}{R_B} b_\alpha^\dagger b_\alpha + \hat{N}_q g_\omega^q \omega(\vec{R}) \cosh\eta + BV \tag{2.33}$$

This choice of the parameter however leads to the eigenfrequency and wavefunction ϕ^α becoming dependent on $\vec{R}$ via the sigma meson field. However, this does also lead to the Hamiltonian gaining a clear physical interpretation, when we act the Hamiltonian on the wavefunction of a nucleon.

When we act this Hamiltonian on a nucleon's wavefunction we find the energy for the nucleon in the IRF. We first begin by noting that we expect the nucleon should be described by three quarks in the lowest energy states. And thus when acting $b_\alpha^\dagger b_\alpha$ on the nucleon, we expect to pick up three factors of Ω_0. Similarly, when acting the number operator on the nucleon, $\hat{N}_q$, we shall pick up a factor of 3 for the 3 valence quarks. This then gives the expression for the energy of a nucleon:

$$E_0^{IRF} = \frac{3\Omega_0(\vec{R})}{R_B} + BV + 3g_\omega^q \omega(\vec{R}) \cosh\eta \tag{2.34}$$

Thus, we find that we have the energy from the 3 valence quarks in the first term, the energy contribution from the ω meson, and also the bag energy from the MIT bag model. From here we shall set the effective mass of the nucleon as:

$$M_N^*(\vec{R}) = \frac{3\Omega_0(\vec{R})}{R_B} + BV \tag{2.35}$$

With this energy, we can now transform back to the NRF, to find the NRF energy:

$$E_0 = M_N^*(\vec{R}) \cosh\eta + 3g_\omega^q \omega(\vec{R}) \tag{2.36}$$

The final step to obtain the classical energy for a nucleon, is to note that this energy can be described by the Lagrangian:

$$L(\vec{R}, \vec{v}) = -M_N^*(\vec{R})\sqrt{1 - v^2} - 3g_\omega^q \omega(\vec{R}) \tag{2.37}$$

And then by performing an expansion in powers of v^2, we find that the non-relativistic expansion is given by:

$$L(\vec{R},\vec{v}) \approx \frac{1}{2}M_N^*(\vec{R})v^2 - M_N^*(\vec{R}) - 3g_\omega^q\omega(\vec{R}) \tag{2.38}$$

Which can be written as the classical Hamiltonian:

$$H_{classical} = \frac{\vec{P}^2}{2M_N^*(\vec{R})} + M_N^*(\vec{R}) + 3g_\omega^q\omega(\vec{R}) \tag{2.39}$$

And so we conclude that the classical energy is given by:

$$\frac{\vec{P}^2}{2M_N^*(\vec{R})} + M_N^*(\vec{r}) + 3g_\omega^q\omega(\vec{R}) \tag{2.40}$$

At this point it is appropriate to consider the ρ meson and it's contribution to the energy. We note that the difference between the ρ and ω is that the ρ is an isovector meson, and so we must account for the isospin factors. However this leaves much of the derivation unchanged, and so we can conclude that we simply need substitute:

$$3g_\omega^q \to g_\rho^q\frac{\tau_3^N}{2} \tag{2.41}$$

Where here the isospin operator is acting on the third component of isospin for the nucleon. Thus we obtain the contribution from the vector mesons to the energy:

$$V(\vec{R}) = 3g_\omega^q\omega(\vec{R}) + g_\rho^q\frac{\tau_3^N}{2}b(\vec{R})(\vec{R}) \tag{2.42}$$

Here, we have chosen b to be the component of the ρ meson, which corresponds to the time component of the ρ meson field, and the $\alpha = 3$ component in isospin space. Thus, we find the classical energy for a nucleon, given as:

$$E_{classical} = \frac{\vec{P}^2}{2M_N^*(\vec{R})} + M_N^*(\vec{r}) + V(\vec{R}) \tag{2.43}$$

Now that we have found the classical energy for a nucleon, we wish to move towards a many-body expansion of the QMC Hamiltonian. By performing this many-body expansion it is possible to find a Hamiltonian which is much easier to compare to the standard nuclear many-body theories. With this the goal is to produce a model with less parameters with a simple relation to the coupling of the meson fields to the quarks, than other models. Before we can get to this however, we must make a digression in order to make clear the definitions of the different couplings in this work.

2.2.1 Coupling Constants

At this point, it is necessary to make clear the meaning of the different coupling constants used throughout this work. It is key to the QMC model that the coupling of the meson fields is to the quarks. The coupling of these fields to the quarks within the baryons is denoted by a superscript, g^q_σ, g^q_ω and g^q_ρ. Next the coupling of the fields to the nucleon can be found from these quark couplings. These are denoted simply by g_σ, g_ω, and g_ρ.

In order to find the relation between these coupling constants we shall consider the solution to the meson-fields in the mean-field approximation. We shall continue to follow the derivation as laid out in Guichon et al 1996 [4].

The equations of motion for the meson field operators are given by:

$$\partial_\mu \partial^\mu \hat{\sigma} + m^2_\sigma \hat{\sigma} = g^q_\sigma \bar{q} q \tag{2.44}$$

$$\partial_\mu \partial^\mu \hat{\omega^\nu} + m^2_\omega \hat{\omega^\nu} = g^q_\omega \bar{q} \gamma^\nu q \tag{2.45}$$

$$\partial_\mu \partial^\mu \rho^{\hat{\nu},\alpha} + m^2_\rho \rho^{\hat{\nu},\alpha} = g^q_\rho \bar{q} \gamma^\nu \frac{\tau^\alpha}{2} q \tag{2.46}$$

From here we consider the mean fields, which are the expectation values of the meson fields in the ground state of the nucleus. We shall represent the ground state of the nucleus as $|A\rangle$, and thus:

$$\langle A| \hat{\sigma}(t, \vec{r}) |A\rangle = \sigma(\vec{r}) \tag{2.47}$$

$$\langle A| \hat{\omega^\nu}(t, \vec{r}) |A\rangle = \delta(\nu, 0)\omega(\vec{r}) \tag{2.48}$$

$$\langle A| \rho^{\hat{\nu},\alpha}(t, \vec{A}) |0\rangle = \delta(\nu, 0)\delta(\alpha, 3) b(\vec{r}) \tag{2.49}$$

From here, must evaluate the source terms in the mean field approximation. For brevity's sake, we shall once again neglect the rho meson term here, as it follows similarly to the derivation of the ω term.

We begin by noting that in the mean field approximation the sources are the sum of the sources created by each nucleon. Thus, we have:

$$\bar{q} q(t, \vec{r}) = \sum_{i=1,A} \langle \bar{q} q(t, \vec{r}) \rangle_i \tag{2.50}$$

$$\bar{q} \gamma^\nu q(t, \vec{r}) = \sum_{i=1,A} \langle \bar{q} \gamma^\nu q(t, \vec{r}) \rangle_i \tag{2.51}$$

We once again note that the nucleons are described in the IRF by 3 quarks in the lowest energy state. Thus, in the IRF of a given nucleon:

$$\langle \bar{q}q(t,\vec{r})\rangle_i = 3\sum_m \bar{\phi}_i^{0,m}(\vec{u'})\phi_i^{0,m}(\vec{u'}) = 3s_i(\vec{u'}) \tag{2.52}$$

$$\langle \bar{q}\gamma^\nu q(t,\vec{r})\rangle_i = 3\delta(\nu,0)\sum_m \phi_i^{\dagger\ 0,m}(\vec{u'})\phi_i^{0,m}(\vec{u'}) = 3\delta(\nu,0)w_i(\vec{u'}) \tag{2.53}$$

Then to evaluate the expectation value for the nucleus in its ground state, we must convert these to the NRF. We find at t in the NRF we have:

$$R'_{i,||} = R_{t,||}\cosh\eta_i - t\sinh\eta_i,\ \vec{R'_{i,\perp}} = \vec{R_{i,\perp}} \tag{2.54}$$

$$r'_{||} = r_{||}\cosh\eta_i - t\sinh\eta_i,\ \vec{r'}_\perp = \vec{r}_\perp \tag{2.55}$$

And thus:

$$u'_{i,||} = (r_{||} - R_{i,||})\cosh\eta_i,\ \vec{u'}_{i,\perp} = \vec{r_\perp} - \vec{R}_{i,\perp} \tag{2.56}$$

So from the Lorentz transformations of these source terms we can find the equations:

$$\langle \bar{q}q(t,\vec{r})\rangle_i = 3s_i((r_{||} - R_{i,||})\cosh\eta_i, \vec{r}_\perp - \vec{R}_{i,\perp})) \tag{2.57}$$

$$\left\langle \bar{q}\gamma^0 q(t,\vec{r})\right\rangle_i = 3w_i((r_{||} - R_{i,||})\cosh\eta_i, \vec{r}_\perp - \vec{R}_{i,\perp}))\cosh\eta_i \tag{2.58}$$

$$\langle \bar{q}\vec{\gamma}q(t,\vec{r})\rangle_i = 3s_i((r_{||} - R_{i,||})\cosh\eta_i, \vec{r}_\perp - \vec{R}_{i,\perp}))\hat{v}_i\sinh\eta_i \tag{2.59}$$

Which, by taking the Fourier transform, can be expressed as:

$$\langle \bar{q}q(t,\vec{r})\rangle_i = \frac{3}{(2\pi)^3}(\cosh\eta_i)^{-1}\int d\vec{k}e^{i\vec{\cdot}(\vec{r}-\vec{R}_i}S(k,\vec{R}_i) \tag{2.60}$$

$$\left\langle \bar{q}\gamma^0 q(t,\vec{r})\right\rangle_i = \frac{3}{(2\pi)^3}\int d\vec{k}e^{i\vec{\cdot}(\vec{r}-\vec{R}_i}W(k,\vec{R}_i) \tag{2.61}$$

$$\langle \bar{q}\vec{\gamma}q(t,\vec{r})\rangle_i = \frac{3}{(2\pi)^3}\vec{v}_i\int d\vec{k}e^{i\vec{\cdot}(\vec{r}-\vec{R}_i}W(k,\vec{R}_i) \tag{2.62}$$

Where the expressions for $S(\vec{k},\vec{R}_i)$ and $W(\vec{k},\vec{R}_i)$ are given by:

$$S(\vec{k},\vec{R}_i) = \int d\vec{u}e^{-i(\vec{k}_\perp\cdot\vec{u}_\perp + k_{||}u_{||}/\cosh\eta_i)}s_i(\vec{u}) \tag{2.63}$$

$$W(\vec{k},\vec{R}_i) = \int d\vec{u}e^{-i(\vec{k}_\perp\cdot\vec{u}_\perp + k_{||}u_{||}/\cosh\eta_i)}w_i(\vec{u}) \tag{2.64}$$

From here, one can show that the mean field expressions for the meson sources are given by:

$$\langle A|\,\bar{q}q(t,\vec{r})\,|A\rangle = \frac{3}{(2\pi)^2}\int d\vec{k}e^{i\vec{k}\cdot\vec{r}}\,\langle A|\,(\cosh\eta_i)^{-1}e^{-i\vec{k}\cdot\vec{R}_i}S(\vec{k},\vec{R}_i\,|A\rangle \tag{2.65}$$

$$\langle A|\,\bar{q}\gamma^0 q(t,\vec{r})\,|A\rangle = \frac{3}{(2\pi)^2}\int d\vec{k}e^{i\vec{k}\cdot\vec{r}}\,\langle A|\,e^{-i\vec{k}\cdot\vec{R}_i}W(\vec{k},\vec{R}_i\,|A\rangle \tag{2.66}$$

$$\langle A|\,\bar{q}\vec{\gamma}q(t,\vec{r})\,|A\rangle = 0 \tag{2.67}$$

The final equation being true as the velocity vector will average to zero. Finally, before obtaining the equations of motion in the mean-field equation, we must consider the matrix elements inside the integrals. We first begin by noting that the elements, $\langle A|\sum_i e^{-i\vec{k}\cdot\vec{R}_i}...\,|A\rangle$ are negligible unless the magnitude of $\vec{k}$ is less than, or on the order of the reciprocal of the nuclear radius. As can be seen in the expressions for $S(\vec{k},\vec{R}_i)$ and $W(\vec{k},\vec{R}_i)$, $\vec{k}$ and $\vec{u}$ are multiplied together, and $\vec{u}$ is bounded by the nucleon radius. This means that provided we are considering appropriately large nuclei, we can neglect the argument of the exponential in the definitions of $S(\vec{k},\vec{R}_i)$ and $W(\vec{k},\vec{R}_i)$.

Then, recognising that $\int d\vec{k}e^{i\vec{k}\cdot(\vec{r}-\vec{R}_i} = \delta(\vec{r}-\vec{R}_i$, and $(\cosh\eta_i)^{-1} = \frac{M_N^*(\vec{R}_i)}{E_i - V(\vec{R}_i)}$ we can define the scalar, vector, and isospin densities:

$$\rho_s(\vec{r}) = \langle A|\sum_i \frac{M_N^*(\vec{R}_i)}{E_i - V(\vec{R}_i)}\delta(\vec{r}-\vec{R}_i)\,|A\rangle \tag{2.68}$$

$$\rho_V(\vec{r}) = \langle A|\sum_i \delta(\vec{r}-\vec{R}_i)\,|A\rangle \tag{2.69}$$

$$\rho_3(\vec{r}) = \langle A|\sum_i \frac{\tau_3^N}{2}\delta(\vec{r}-\vec{R}_i)\,|A\rangle \tag{2.70}$$

Then the expectation values of the source terms are given the forms, deducing what the isovector term should be from the ω derivation:

$$\langle A|\,\bar{q}q(t,\vec{r})\,|A\rangle = 3S(\vec{r})\rho_s(\vec{r}) \tag{2.71}$$

$$\langle A|\,\bar{q}\gamma^\nu q(t,\vec{r})\,|A\rangle = 3\delta(\nu,0)\rho_V(\vec{r}) \tag{2.72}$$

$$\langle A|\,\bar{q}\gamma^\nu\frac{\tau^\alpha}{2}q(t,\vec{r})\,|A\rangle = \delta(\nu,0\delta(\alpha,3)\rho_3(\vec{r}) \tag{2.73}$$

Where here we have $S(\vec{r})$ as:

$$S(\vec{r}) = S(0,\vec{r}) = \int d\vec{u} s_{\vec{r}}(\vec{u}) \tag{2.74}$$

$$= \frac{\Omega_0/2 + m_q^* R_B(\Omega_0 - 1)}{\Omega_0(\Omega_0 - 1) + m_q^* R_B/2} \tag{2.75}$$

Finally, we can find the mean fields equations for the meson fields, and from here deduce the relationship between the nucleon and quark coupling constants for the different meson fields. We find:

$$(-\nabla_r^2 + m_\sigma^2)\sigma(\vec{r}) = g_\sigma S(\vec{r})/S(\sigma = 0)\rho_s(\vec{R}) \tag{2.76}$$

$$(-\nabla_r^2 + m_\omega^2)\omega(\vec{r}) = g_\omega \rho_V(\vec{r}) \tag{2.77}$$

$$(-\nabla_r^2 + m_\rho^2)b(\vec{r}) = g_\rho \rho_3(\vec{r}) \tag{2.78}$$

From here, we can deduce the relation between the nucleon couplings, g_σ, g_ω and g_ρ and their corresponding quark couplings, g_σ^q, g_ω^q, and g_ρ^q:

$$g_\sigma = 3g_\sigma^q S(\sigma = 0) \tag{2.79}$$

$$g_\omega = 3g_\omega^q \tag{2.80}$$

$$g_\rho = g_\rho^q \tag{2.81}$$

We note then that the σ nucleon coupling depends on the quantity $S(\vec{r})$, which will be important in chapter [6].

2.3 Energy Density Functional

With the definitions for the quark couplings clear, we are now ready to work towards the many-body expansion for the QMC Hamiltonian.

$$E_{classical} = \frac{\vec{P}^2}{2M_N^*(\vec{R})} + M_N^*(\vec{R}) + V(\vec{R}) \tag{2.82}$$

Where $V(\vec{R})$ includes the relevant interactions we are concerned with. From here we shall follow closely the derivation from Guichon & Thomas [8], which will ultimately lead to a many-body expansion of the QMC model. We first note that a good approximation can be made for the effective mass:

$$M_N^*(\vec{R}) \approx M_N - g_\sigma \sigma(\vec{R}) + \frac{d}{2}(g_\sigma \sigma(\vec{R}))^2 \tag{2.83}$$

Here, d is the scalar polarizability, which functions analogously to the electric or magnetic polarizability in electromagnetism. It is a parameter which is fitted to reproduce the correct nucleon mass [41], and has units of [fm]. One can also make a good approximation for the momentum term, by taking a Taylor expansion of the effective mass. Then combining these approximations together, we find:

$$\frac{\vec{P}^2}{2M_N^*(\vec{R})} + M_N^*(\vec{R}) \approx M_N + \frac{\vec{P}^2}{2M_N} - g_\sigma\sigma(\vec{R}) \times \left[1 - \frac{d}{2}g_\sigma\sigma(\vec{R})\right] \times \left(1 - \frac{\vec{P}^2}{2M_N^2}\right) \quad (2.84)$$

Combining these two approximations together we find:

$$E_{classical} = \frac{\vec{P}^2}{2M_N} + M_N - g_\sigma\sigma(\vec{R})\left[1 - \frac{d}{2}g_\sigma\sigma(\vec{R})\right] \times \left[1 - \frac{\vec{P}^2}{2M_N^2}\right] + V(\vec{R}) \quad (2.85)$$

And thus we have obtained the classical energy for a single nucleon, in a useful form for our work here. Then, we can write down the energy density functional, by including the energy from the meson fields, and summing over all the nucleons in the system:

$$E = \sum_i E_{N,i} + E_{meson} \quad (2.86)$$

Where E_{meson} is given by:

$$E_{meson} = \frac{1}{2}\int d^3r \left[(\vec{\nabla}\sigma)^2 + m_\sigma^2\sigma^2\right] - \frac{1}{2}\int d^3r \left[(\vec{\nabla}\omega)^2 + m_\omega^2\omega^2 + (\vec{\nabla}\rho)^2 + m_\rho^2 b^2\right] \quad (2.87)$$

However we note that it is not particularly useful to have the nucleon energy in the form $\sum_i E_{N,i}$, and it will be much more useful to express this in terms of the nucleon density. This can be done, by expressing the density as:

$$\rho^{cl}(\vec{r}) = \sum_i \delta(\vec{r} - \vec{R}_i) \quad (2.88)$$

And then for the scalar density, which includes the velocity-dependent term, we will express for now as:

$$\rho_s^{cl}(\vec{r}) = \sum_i \delta(\vec{r} - \vec{R}_i) \times \left[1 - \frac{\vec{P}_{iN}^{\,2}}{2M_N^2}\right] \quad (2.89)$$

And so we can then replace the sums over the nucleons with integrals over the nucleon densities, as below:

$$\int d^3r\rho^{cl}(\vec{r})g_\omega\omega(\vec{r}) = \sum_i g_\omega\omega(\vec{R}_i) \tag{2.90}$$

$$\int d^3r(\vec{r})\left[g_\sigma\sigma(\vec{r}) - \frac{d}{2}(g_\sigma\sigma(\vec{r}))^2\right]\rho_s^{cl} = \sum_i \left[g_\sigma\sigma(\vec{R}_i) - \frac{d}{2}(g_\sigma\sigma(\vec{R}_i))^2\right]\left[1 - \frac{\vec{P}_{iN}^{\,2}}{2M_N^2}\right] \tag{2.91}$$

And so the energy density functional can be expressed as:

$$E = \sum_i \left[M + \frac{\vec{P}_{iN}^{\,2}}{2M_N}\right] + E_{meson} - \int d^3r(\vec{r})\left[g_\sigma\sigma(\vec{r}) - \frac{d}{2}(g_\sigma\sigma(\vec{r}))^2\right]\rho_s^{cl} + \int d^3r\rho^{cl}(\vec{r})g_\omega\omega(\vec{r}) \tag{2.92}$$

2.4 Meson Field Equations of Motion

With the energy density functional obtained in this form, it is now possible to solve for the equations of motion for the meson fields. These are defined by the functional derivatives:

$$\frac{\delta E}{\delta\sigma} = 0 \tag{2.93}$$

$$\frac{\delta E}{\delta\omega} = 0 \tag{2.94}$$

Where once again the ρ meson is treated similarly to the ω and so we shall neglect for now, and reintroduce it again towards the end of this section.

Then taking the functional derivative with respect to the meson fields, we obtain the equations of motion for the meson fields:

$$\frac{\delta E}{\delta\sigma} = 0 = -\vec{\nabla}^2\sigma - m_\sigma^2\sigma + \rho_s^{cl}g_\sigma\sigma\left[1 - dg_\sigma\sigma\right] \tag{2.95}$$

$$\frac{\delta E}{\delta\omega} = 0 = -\vec{\nabla}^2\omega - m_\omega^2\omega + g_\omega\rho^{cl} \tag{2.96}$$

Now if we define $G_\sigma = g_\sigma^2/m_\sigma^2$, and $G_\omega = g_\omega^2/m_\omega^2$, the equations can be expressed as:

$$g_\sigma\sigma = G_\sigma(1 - dg_\sigma\sigma)\rho_s^{cl} + \nabla^2\frac{g_\sigma\sigma}{m_\sigma^2} \tag{2.97}$$

$$g_\omega\omega = G_\omega\rho^{cl} + \nabla^2\frac{g_\omega\omega}{m_\omega^2} \tag{2.98}$$

In these equations, let us first consider the derivative terms. It is assumed that the meson fields will follow roughly the nucleon density, and that the scale of the derivative operator will be the thickness of the nuclear surface, roughly a few [fm]. Thus, it is reasonable to treat the terms containing these derivatives as perturbations and thus replace the fields in these equations with the nucleon density. So, we shall use $g_\sigma\sigma \approx G_\sigma\rho_s^{cl}$ or $g_\omega\omega \approx G_\omega\rho^{cl}$ for these terms.

With this substitution we note that the ω meson field equation becomes:

$$g_\omega\omega_{sol} = \frac{G_\omega}{m_\omega^2}\nabla^2\rho^{cl} + G_\omega\rho^{cl} \tag{2.99}$$

And hence the solution to this has been found with that substitution. Then the analogous solution to the ρ meson would be:

$$g_b b_{sol} = \frac{G_b}{m_b^2}\nabla^2\rho^{cl} + G_b\frac{\tau_3}{2}\rho^{cl} \tag{2.100}$$

With solutions to both the ω and ρ meson fields, we now turn to the σ meson field.

2.4.1 Sigma meson equation of motion

The simplest way to solve for the σ meson field is to find an iterative solution. As we expect the meson fields to go like the nucleon density, we begin by taking the lowest order approximation:

$$g_\sigma\sigma = G_\sigma\rho_s^{cl} \tag{2.101}$$

We then substitute this into the equation of motion, to find:

$$g_\sigma\sigma^1 = \frac{G_\sigma}{m_\sigma^2}\nabla^2\rho_s^{cl} + G_\sigma(\rho_s^{cl})^2(1 - dG_\sigma\rho_s^{cl}) \tag{2.102}$$

Then one can repeat this substitution, to generate higher order many body terms. So, the solution to the σ meson field, to an arbitrary order of many body forces, is given by:

$$g_\sigma\sigma_{sol} = \frac{G_\sigma}{m_\sigma^2}\nabla^2\rho_s^{cl} + G_\sigma\rho_s^{cl} + \sum_{j\geq 1}(-d)^j(G_\sigma\rho^c l_s)^{j+1} \tag{2.103}$$

2.5 Many-Body Hamiltonian

With solutions to the meson field equations, the final step in this derivation, is to substitute these solutions back into the energy-density functional, to obtain a many-body expansion of the QMC model Hamiltonian. Here, for the sake of brevity, we shall only consider terms up to and including three-body interactions, though it is a simple process to generate higher order many-body interactions, by repeatedly iterating the meson field equations. We shall also neglect the spin-orbit interactions here too. This results in a Hamiltonain of the form:

$$H_{QMC} = \sum_i \frac{\vec{P}_i^2}{2M} + \int d^3r \left[-\frac{G_\sigma}{2}\rho^2 + \frac{dG_\sigma^2}{2}\rho^3 + \frac{G_\sigma \vec{P}^2}{2M^2}\rho^2 - \frac{G_\sigma}{2m_\sigma^2}\rho\nabla^2\rho + \mathcal{O}(\rho^4) \right] + \int d^3r \left[\frac{G_\omega}{2}\rho^2 + \frac{G_\omega}{2m_\omega^2}\rho\nabla^2\rho + \frac{G_\rho}{2}\frac{\vec{\tau}_i \cdot \vec{\tau}_j}{4}\left(\rho^2 + \frac{1}{m_\rho^2}\rho\nabla^2\rho\right) \right] \quad (2.104)$$

And thus a simple many-body expansion of the Hamiltonian for the QMC model has been found. This enables us to compare the results from the QMC model to those from other models, to compare the effectiveness of them.

Chapter 3

Lambda Nucleon Many-Body Forces

Compared to the other hyperons, the binding data for the Λ is relatively abundant. This makes the Λ binding ideal for fitting the σ and ω meson coupling constants, before we turn to making the prediction for Ξ hyperon binding energies. To get to fitting these constants, first the many-body forces expansion will be extended to include Λ hyperons. From this, the potential energy can be formulated for the binding of the Λ in a nucleus. With this potential it is possible to write down the Schrödinger equation, and solve an eigenvalue problem to find the binding energy. This was accomplished by using the numerov algorithm. Finally the best fit will be carried out including 3, 4, or 5 body forces, to determine which provides the best fit.

3.1 Finding the Many-Body forces

In chapter [2], the derivation for the many body forces for nucleon-nucleon interactions was presented. This can now be extended to include the interactions between the Λ and nucleons. First, the classical energy must be defined. This is done in an analogous way to the classical energy of the nucleon. Now, as seen in table [1.2], we note that the Λ, has zero isospin, and hence does not interact with the ρ meson, and is electrically neutral, so does not experience the Coulomb potential. Thus, for a given Λ hyperon located at $\vec{R}_j$, the classical energy is given by:

$$E_{\Lambda j} = \frac{\vec{P}_j^{\,2}}{2M^*_\Lambda(\vec{R}_j)} + M^*_\Lambda(\vec{R}_j) + g_\omega\omega(R_j) + V_{so} \tag{3.1}$$

We will apply the same expansion to the effective mass, as seen in the derivation for nucleon-nucleon interactions, and so we can expand the classical energy in terms of the σ field as:

$$E_{\Lambda j} = M_\Lambda - g_\sigma \sigma \left[w - \frac{\tilde{w} d}{2} g_\sigma \sigma \right] \times \left[1 - \frac{\vec{P}_j^2}{2M_\Lambda^2} \right] + \frac{\vec{P}_j^2}{2M_\Lambda} + g_\omega \omega(\vec{R}_j) \tag{3.2}$$

It is worth noting, that here we neglect the spin-orbit interaction, as it does not significantly contribute to the many-body forces, and is small regardless for Λ hypernuclei [40]. This accords with what has been previously shown in the QMC model, where the spin-orbit interactions in hypernuclei have been shown to be small [17] [42]. Here, the constants w and $\tilde{w}$, are fit to reproduce the Λ mass in-medium [41].

Now the total energy density functional can be defined as:

$$E_{QMC} = \sum_i E_{Ni} + \sum_j E_{\Lambda j} + E_{meson} \tag{3.3}$$

And as before, we will replace $\rho^{cl} = \sum_j \delta(\vec{r} - \vec{r_j'})$, and so turn this expression into an integral expression, as shown below:

$$\begin{aligned} E_{QMC} = &\sum_i \frac{\vec{P_i}^2}{2M_N} + \sum_j \frac{\vec{P_j}^2}{2M_\Lambda} - \int dV \rho_N g_\sigma \sigma \left[1 - \frac{d}{2} g_\sigma \sigma \right] \times \left[1 - \frac{P_N^2}{2M_N^2} \right] \\ &- \int dV \rho_\Lambda g_\sigma \sigma \left[w - \frac{\tilde{w} d}{2} g_\sigma \sigma \right] \times \left[1 - \frac{P_\Lambda^2}{2M_\Lambda^2} \right] + \int dV g_\omega \omega \left[\rho_N(\vec{r}) + w_\omega \rho_\Lambda(\vec{r}) \right] + E_{meson} \end{aligned} \tag{3.4}$$

Where the weighting for the ω meson is $w_\omega = 1 + \frac{S_B}{3}$ and s_B is the strangeness of the baryon, and so here, as we are considering a Λ, this is given by $w_\omega = \frac{2}{3}$. In addition, E_{meson} is given by:

$$E_{meson} = \frac{1}{2} \int dV \left[(\vec{\nabla}\sigma)^2 + m_\sigma^2 \sigma^2 \right] - \frac{1}{2} \int dV \left[(\vec{\nabla}\omega)^2 + m_\omega^2 \omega^2 \right] \tag{3.5}$$

With this it is now possible to find the equations of motion for the meson fields, and thus form a Hamiltonian which can be used to explore nuclear phenomena.

3.2 Equations of Motion

From here it is now possible to find the equations of motion for the mesons, by varying the energy density functional, as before. Thus we obtain:

$$\frac{\delta E}{\delta \sigma} = 0 = -\vec{\nabla}^2\sigma - m_\sigma^2\sigma + \rho_N g_\sigma \sigma \left[1 - d g_\sigma \sigma\right] + \rho_\Lambda g_\sigma \sigma \left[w - \tilde{w} d g_\sigma \sigma\right] \times \left[1 - \frac{P_\Lambda^2}{2M_\Lambda^2}\right] \tag{3.6}$$

$$\frac{\delta E}{\delta \omega} = 0 = -\vec{\nabla}^2\omega - m_\omega^2\omega + g_\omega(\rho_N + w_\omega \rho_\Lambda) \tag{3.7}$$

Which taking $G_\sigma = \frac{g_\sigma^2}{m_\sigma^2}$ and $G_\omega = \frac{g_\omega^2}{m_\omega^2}$, these equations can be simplified, as:

$$g_\sigma \sigma = -\frac{g_\sigma}{m_\sigma^2}\vec{\nabla}^2\sigma + \rho_N G_\sigma \sigma \left[1 - d g_\sigma \sigma\right] + \rho_\Lambda G_\sigma \sigma \left[w - \tilde{w} d g_\sigma \sigma\right] \times \left[1 - \frac{P_\Lambda^2}{2M_\Lambda^2}\right] \tag{3.8}$$

$$g_\omega \omega = -\frac{g_\omega}{m_\omega^2}\vec{\nabla}^2\omega + G_\omega(\rho_N + w_\omega \rho_\Lambda) \tag{3.9}$$

Now in order to solve the sigma equation, we will make use of an iterative approach. We will apply a similar approximation as to that before, where here we have:

$$g_\sigma \sigma^0 = G_\sigma \rho_N + w G_\sigma \rho_\Lambda \tag{3.10}$$

Upon substituting this into the equations of motion to obtain the first iteration we find:

$$\begin{aligned} g_\sigma \sigma^1 = -\frac{1}{m_\sigma^2}\vec{\nabla}^2 \left[G_\sigma \rho_N + w G_\sigma \rho_\Lambda\right] + G_\sigma \rho_N (1 - d[G_\sigma \rho_N + w G_\sigma \rho_\Lambda]) \\ + G_\sigma \rho_\Lambda (w - \tilde{w} d[G_\sigma \rho_N + w G_\sigma \rho_\Lambda]) \left[1 - \frac{P_\Lambda^2}{2M_\Lambda^2}\right] \end{aligned} \tag{3.11}$$

And upon making a similar substitution for the ω equation:

$$g_\omega \omega = -\frac{1}{m_\omega^2}\vec{\nabla}^2 \left[G_\omega \rho_N + w G_\omega \rho_\Lambda\right] + G_\omega \rho_N + w_\omega G_\omega \rho_\Lambda \tag{3.12}$$

Now with solutions to the equations of motion at hand, one can substitute these equations into the energy density functional, to find a Hamiltonian dependent on the density of the nuclear material, and not the meson fields. For the sake of brevity, only terms containing a ρ_Λ will be included below, as the binding of a single Λ hyperon into a nucleon is being investigated. Thus, the contribution from the sigma meson is given by:

$$H_\sigma^{(\Lambda)} = \rho_\Lambda \Bigg\{ \frac{-wdG_\sigma^2}{m_\sigma^2}(\vec{\nabla}\rho_N)^2 + \frac{wd^2G_\sigma^3}{m_\sigma^2}(\vec{\nabla}(\rho_N^2)) \cdot (\vec{\nabla}\rho_N) + \\ \Bigg[-G_\sigma w \rho_N + \left(w + \frac{\tilde{w}}{2}\right) dG_\sigma^2 \rho_N^2 - (w+\tilde{w})\, d^2 G_\sigma^3 \rho_N^3 - \frac{\tilde{w}dG_\sigma^2}{m_\sigma^2}(\vec{\nabla}\rho_N)^2 \\ + \frac{\tilde{w}d^2G_\sigma^3}{m_\sigma^2}(\vec{\nabla}(\rho_N^2)) \cdot (\vec{\nabla}\rho_N) + \frac{G_\sigma^3\rho_N^2 d^2(w+2\tilde{w})}{m_\sigma^2}(\nabla^2\rho_N) \Bigg] \times \left(1 - \frac{\vec{P_\Lambda}^{\,2}}{2M_\Lambda^2}\right) \Bigg\} \tag{3.13}$$

Above, terms including $(1/m_\sigma^2)^2$ are ignored, as these terms are small enough to be negligible compared to the others. In addition terms including $\nabla\rho_\Lambda$ are also not included. The term for the ω meson, neglecting all the derivative terms for the same reason as above, is given by:

$$H_\omega = G_\omega w_\omega \rho_N \rho_\Lambda \tag{3.14}$$

This contributes a repulsive component to the many-body forces. We note that this two-body interaction is the highest order that the omega meson contributes to the many-body forces.

3.3 Calculating the Binding Energy

With the Hamiltonian determined, it is now possible to calculate the binding energy. This can be accomplished by solving the energy-eigenvalue problem for the Schrödinger equation:

$$H\Psi_\Lambda = E\Psi_\Lambda \tag{3.15}$$

In order to obtain this equation, the variation of the full Hamiltonian, with respect to ρ_Λ is taken, and terms containing any remaining factors of ρ_Λ are neglected. These terms containing remaining factors of ρ_Λ are neglected as there is only one Λ present in the nuclear environment, and so there are no $\Lambda\Lambda$ interactions. This returns the equations of motion for a single Lambda bound into the nuclear environment via the many-body interaction.

From here it is possible to set up the Schrödinger equation. The equation of motion found from the Hamiltonian gives a Schrödinger equation of the form:

$$\frac{\vec{P_\Lambda}^{\,2}}{2M_\Lambda}\Psi(\vec{r}) + G_\omega w_\omega \rho_N \Psi(\vec{r}) + \left[-G_\sigma w \rho_N + \left(w + \frac{\tilde{w}}{2}\right) d G_\sigma^2 \rho_N^2 - (w + \tilde{w})\, d^2 G_\sigma^3 \rho_N^3\right]\left(1 - \frac{\vec{P_\Lambda}^{\,2}}{2M_\Lambda^2}\right)\Psi(\vec{r}) = E\Psi(\vec{r}) \tag{3.16}$$

Now the terms from the sigma equation that include momentum dependence are the velocity-dependent corrections. Grouping all these terms with the $\frac{\vec{P_\Lambda}^{\,2}}{2M_\Lambda}$, and making the usual substitution $\vec{P_\Lambda} = -i\vec{\nabla}$ (working in units $\hbar = 1$), this can be rearranged as:

$$-\left[1 + \frac{1}{M_\Lambda} G_\sigma w \rho_N - \frac{1}{M_\Lambda}\left(w + \frac{\tilde{w}}{2}\right) d G_\sigma^2 \rho_N^2 + \frac{1}{M_\Lambda}(w + \tilde{w})\, d^2 G_\sigma^3 \rho_N^3\right]\frac{\nabla^2}{2M_\Lambda}\Psi(\vec{r}) + \left[G_\omega w_\omega \rho_N - G_\sigma w \rho_N + \left(w + \frac{\tilde{w}}{2}\right) d G_\sigma^2 \rho_N^2 - (w + \tilde{w})\, d^2 G_\sigma^3 \rho_N^3\right]\Psi(\vec{r}) = E\Psi(\vec{r}) \tag{3.17}$$

From here velocity-dependent terms will be collectively labelled as $\eta(r)$, and the other terms will be labelled $V_{binding}(r)$, to shorthand the expressions, such that the equation can be expressed as:

$$-\eta(r)\frac{\vec{\nabla}^2}{2M_\Lambda}\Psi(\vec{r}) + V_{binding}(r)\Psi(\vec{r}) = E\Psi(\vec{r}) \tag{3.18}$$

Where:

$$V_{binding}(r) = G_\omega w_\omega \rho_N - G_\sigma w \rho_N + \left(w + \frac{\tilde{w}}{2}\right) d G_\sigma^2 \rho_N^2 - (w + \tilde{w})\, d^2 G_\sigma^3 \rho_N^3 \tag{3.19}$$

$$\eta(r) = 1 + \frac{1}{M_\Lambda} G_\sigma w \rho_N - \frac{1}{M_\Lambda}\left(w + \frac{\tilde{w}}{2}\right) d G_\sigma^2 \rho_N^2 + \frac{1}{M_\Lambda}(w + \tilde{w})\, d^2 G_\sigma^3 \rho_N^3 \tag{3.20}$$

It is now necessary to find a form for the nucleon density. Throughout it will be assumed that the nucleon density is spherically symmetric, and thus the Hamiltonian will also be spherically symmetric. Second, we will consider the nature of the density of nucleons, which was considered in section [3.2]. Through the majority of this project, the density of nucleons will be represented by a Woods-Saxon density, which is given by the form:

$$\rho_N(r) = \frac{\rho_0}{[1 + \exp((r - cA^{1/3})/a)]} \tag{3.21}$$

This density is plotted for a variety of different nucleus sizes in figure [3.1]. In this equation, the constants in this density to consider are ρ_0 which is the nuclear saturation density throughout taken as $\rho_0 = 0.15[\text{fm}^{-3}]$, and the parameters of the model, which are set to $c = 1.1[\text{fm}]$ and $a = 0.6[\text{fm}]$.

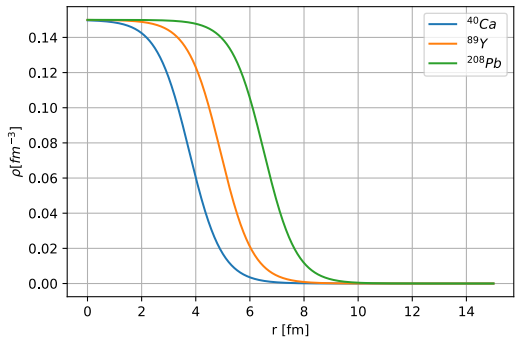

Figure 3.1: Density plotted for a few different nuclei

With this, we now have all that we need to investigate what this binding potential looks like. Plotted in figures [3.2a]-[3.2d] is the 4-body potential with and without correction terms. Included first is a plot with no corrections from the velocity-dependent terms, or the derivatives of the potential, as in figure [3.2a]. Following this a plot is included with all the corrections in figure [3.2b]. Following this a plot of the potential with no derivative corrections [3.2c]. Finally a plot of the derivative contribution is included on its own in figure [3.2d].

Now we will return to expanding the ∇^2 term, in spherical coordinates, and utilising the symmetries of the problem, so as to express the equation in a form which can be solved. As the potential is spherically symmetric, one can first assume assume a separable solution, of the form $\Psi(\vec{r}) = Y_{lm}(\theta, \phi)\psi(r)$, where $Y_{lm}(\theta, \phi)$ are the spherical harmonic functions. Thus, substituting in $\vec{\nabla}^2$ in spherical coordinates, we find:

$$-\frac{1}{2M_\Lambda}\left[\frac{1}{r^2}\frac{\partial}{\partial r}\left(r^2\frac{\partial}{\partial r}\right)\psi(r) - \frac{l(l+1)}{r^2}\psi(r)\right] + \frac{V_{binding}(r)}{\eta(r)}\psi(r) = \frac{E}{\eta(r)}\psi(r) \tag{3.22}$$

Now upon substituting $\psi(r) \to \frac{u(r)}{r}$, and substituting into this equation, one can show:

$$\frac{1}{r^2}\frac{d}{dr}\left(r^2\frac{d}{dr}\right)\frac{u(r)}{r} = \frac{1}{r}\frac{d^2u}{dr^2} \tag{3.23}$$

And thus, making use of this the equation can be expressed as:

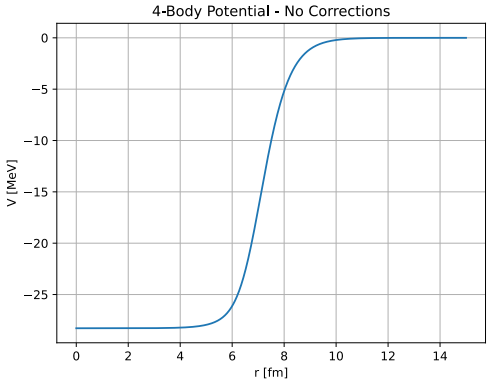

(a) 4-Body Potential without any Corrections

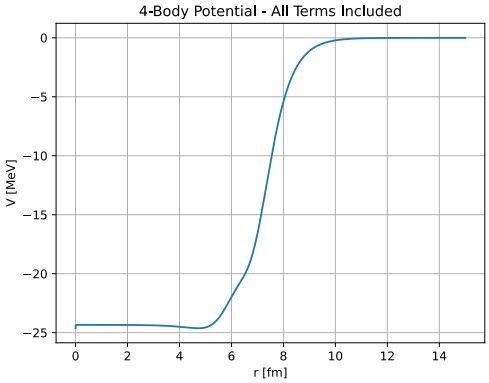

(b) 4-Body Potential including all corrections

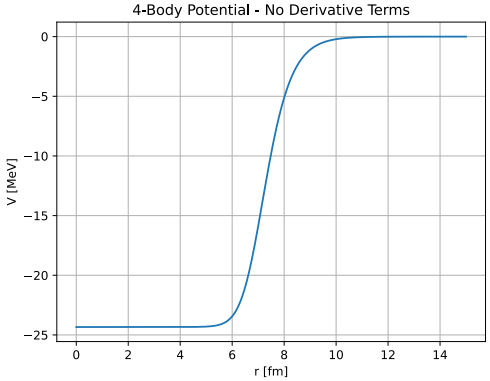

(c) 4-Body Potential with velocity-dependent terms

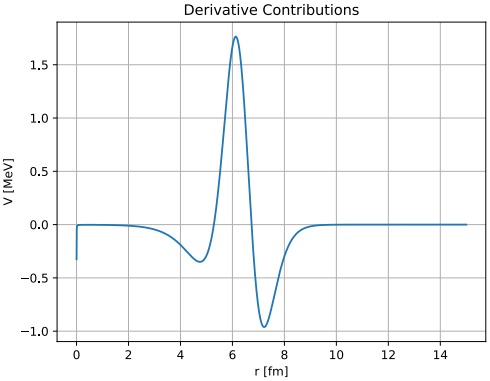

(d) Derivative Contributions to the Binding Potential

Figure 3.2: The 4-Body Potential with and without the derivative and velocity-dependent corrections

$$-\frac{1}{2M_\Lambda}\left[\frac{d^2u}{dr^2}-\frac{l(l+1)}{r^2}u(r)\right]+\frac{V_{binding}(r)}{\eta(r)}u(r)=\frac{E}{\eta(r)}u(r) \tag{3.24}$$

Thus, this equation can be expressed in the form, $\frac{d^2u}{dr^2}=f(r)u(r)$, as shown below:

$$\frac{d^2u}{dr^2}=-2M_\Lambda\left[\frac{1}{\eta(r)}[E-V_{binding}(r)]-\frac{l(l+1)}{2M_\Lambda r^2}\right]u(r) \tag{3.25}$$

With this equation, it is now possible to find $r\psi$, by solving this eigenvalue problem. This is done using the Numerov algorithm. The details of this algorithm and it's

implementation in solving the Schrödinger equation can be found in appendix [A]. The code used can be found at: github.com/NathanaelBotten/MPhil-Code.

3.4 Fitting the Coupling Constants

With a method to find the solution to the Schrödinger equation, and hence the ground state energy, for any given nucleus, it is now of interest to determine which coupling constants provide the best fit to the experimental data. As the Λ has no isospin-dependent interaction, nor any electromagnetic interactions, it is simple enough to run a best fit over a variety of values of G_σ and G_ω. The values chosen were based on previous results from the QMC model, within the bound of plus or minus 10% [35]. So, the values tested were $G_\sigma \in [8.65, 10.60]$ and $G_\omega \in [4.71, 5.70]$. This range was chosen because the many-body expansion is an approximation to the exact solution of the mean fields, and the nucleon density is also an approximation here. Thus, we cannot expect that the coupling constants will be exactly the same here. These constants were tested with step sizes of 0.01, for all the combinations of these constants. The experimental values of the binding energies fitted to, came from Hashimoto and Tamura [11], Gal et al. [43], and Pal et al. [44]. The fit was to the 1s and 1p states for ^{208}Pb, ^{139}La, ^{89}Y, ^{51}V, ^{40}Ca, and ^{32}S. This fit was run with the potential including up to 3-body, 4-body and 5-body interactions. The results of these fits are plotted in figures [3.3a], [3.3b], and [3.3c].

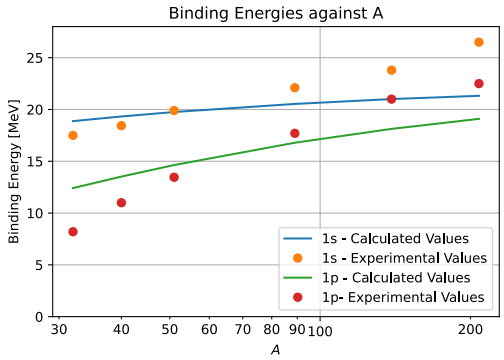

(a) The best fit including 3-body terms

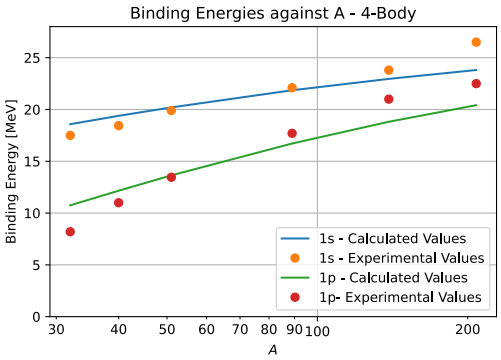

(b) The best fit including 4-body terms

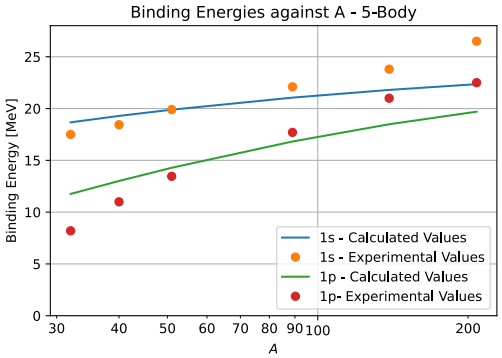

(c) The best fit including 5-body terms

Figure 3.3: The different best fits, including different many-body forces

The 3-body fit yielded the values for the best fit of $G_\sigma = 8.65$, and $G_\omega = 4.96$, with the error $\chi^2 = 5.4008$. The 4-body fit returned a much better fit, with the coupling constants $G_\sigma = 8.65$, and $G_\omega = 5.64$, and an error to the fit $\chi^2 = 1.8190$. Including the 5-body had the effect of reducing the accuracy of the fit, with the error being $\chi^2 = 3.6398$, corresponding to coupling constants $G_\sigma = 8.65$ and $G_\omega = 5.51$. And so we have determined that the best fit is produced by the 4-body model. Hence, when calculating the following, we will continue with this model.

This is peculiar for nuclear physics, as in the vast majority of work a two-body or three-body model is preferred. In these models, four body interactions contribute a relatively small amount to the binding energy, compared to the two and three body interactions [45] [46]. However, we find here that this is not the case here! As can be seen in the plot breaking up the binding potential for ^{208}Pb into its various components, figure [3.4], the two and three body potentials have a difference of approximately 10[MeV]. But the contribution from the 4-body potential is greater than 15[MeV]. This means that in the model laid out above, the 4-body interactions make a significant contribution to the binding energy of the Hyperon! It has been shown previously that the Lambda binding depth is around 26.5[MeV] [13]. Here, adding the 4-body interactions leads to a binding depth much closer than that, so it is sensible that including the 4-body interactions improves the fit to the energies.

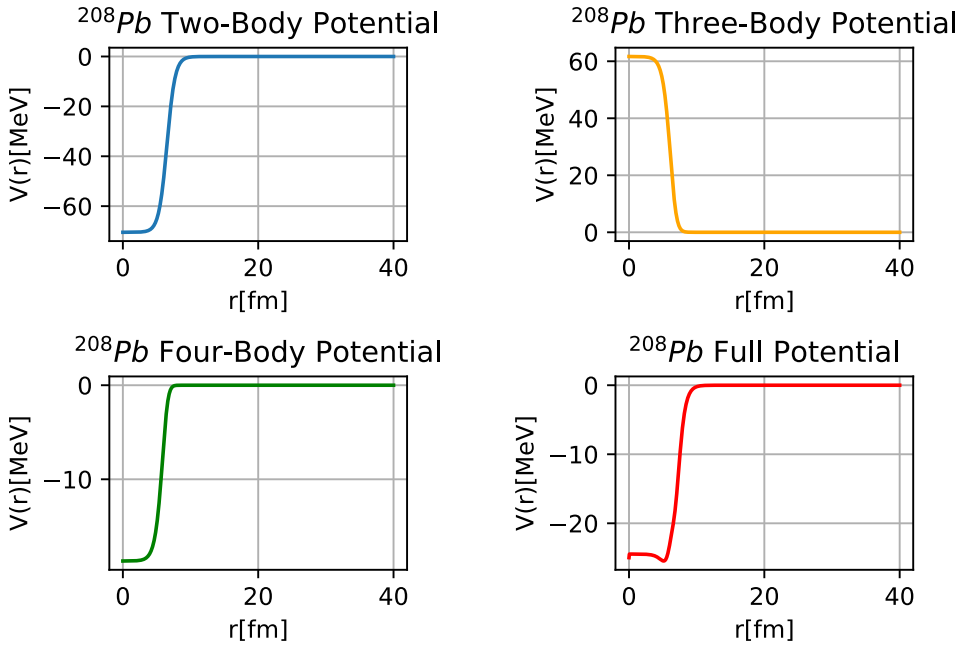

Figure 3.4: Potential split into different many-body forces for ^{208}Pb

Chapter 4

Cascade Nucleon Many-Body Forces

With the best fit for the coupling constants fitted to the binding of the Λ hyperons, we are now in a position to investigate the binding of cascade hyperons. Cascade hyperons come in two varieties. The neutral cascade, Ξ^0, which has the valence quarks uss, and the negative cascade, Ξ^-, which has the valence quarks dss. Thus we note that unlike the Λ^0 hyperon, there will also be an isospin interaction, as the cascade hyperons have isospin $I_z = \pm\frac{1}{2}$. In addition to this the Ξ^- will experience an electromagnetic interaction, which must also be accounted for when calculating the binding energy.

4.1 Deriving the Many-Body Forces

We begin by considering the classical energy of the cascade hyperons. For now we shall neglect the electromagnetic interaction for the Ξ^- hyperon. Thus we have:

$$E_{\Xi k} = \frac{\vec{P_k}^2}{2M^*_\Xi(\vec{R_k})} + M^*_\Xi(\vec{R_k}) + g^\Xi_\omega\omega(\vec{R_k}) + g^\Xi_\rho b(\vec{R_K})\frac{\tau_3}{2} \tag{4.1}$$

Where we have denoted the time component of the ρ meson field with b for the isospin interaction. We also have τ here as the Pauli matrices. This also follows for the nucleon as well, so we have:

$$E_{Ni} = \frac{\vec{P_i}^2}{2M^*_N(R_i)} + M^*_N(\vec{R_i}) + g^N_\omega\omega(\vec{R_i}) + g^N_\rho b(\vec{R_k})\frac{\tau_3}{2} \tag{4.2}$$

We shall treat the effective mass in a similar way as before, so we simplify the classical energy of the cascade hyperon as:

$$E_{\Xi k} = M_\Xi - g_\sigma\sigma\left[w_\Xi - \frac{\tilde{w_\Xi} d}{2} g_\sigma\sigma\right] \times \left[1 - \frac{P_k^2}{2M_\Xi^2}\right] + \frac{P_k^2}{2M_\Xi} + g_\omega^\Xi \omega(R_k) + g_\rho^\Xi b(R_k) \cdot \frac{\tau_3}{2} \quad (4.3)$$

The weightings for the σ field are once again taken from [41], this time with the fitting being to that of the Ξ hyperons. Now, with the classical energy we can calculate the equations of motion.

4.2 Equations of Motion for the Cascade

The process for finding the σ and ω fields is very similar to that of the Λ as in chapter [3], where the significant difference is the coupling constants are adjusted differently. Thus, this part of the derivation will be brief with more depth when considering the isospin and electromagnetic interactions.

4.2.1 σ and ω equations of motion

The equations for the σ and ω proceed in much the same way as they did for the Λ hyperon. We express the σ component of the energy density functional as:

$$E_\sigma = \int dV \left[(\vec{\nabla}\sigma)^2 + m_\sigma^2\sigma^2\right] - \int dV \rho_N g_\sigma\sigma \left[1 - \frac{d}{2} g_\sigma\sigma\right] \times \left[1 - \frac{P_N^2}{2M_N^2}\right] - \int dV \rho_\Xi g_\sigma\sigma \left[w_\Xi - \frac{\tilde{w_\Xi} d}{2} g_\sigma\sigma\right] \times \left[1 - \frac{P_\Xi^2}{2M_\Xi^2}\right] \quad (4.4)$$

Where the equation differs from the Λ case is the fitting constants w and $\tilde{w}$, as these take a different value here to fit the mass of the cascade hyperons. However this does not change the derivation in any substantial way.

Thus, considering terms only of order $\mathcal{O}(\rho_\Xi)$, and excluding the derivative terms here, we find:

$$H_\sigma = \left[-G_\sigma w_\Xi \rho_N \rho_\Xi + \left(w_\Xi + \frac{\tilde{w_\Xi}}{2}\right) d G_\sigma^2 \rho_N^2 \rho_\Xi - (w_\Xi + \tilde{w_\Xi})\, d^2 G_\sigma^3 \rho_N^3 \rho_\Xi\right] \left(1 - \frac{\vec{P_\Xi}^{\,2}}{2M_\Xi^2}\right) \quad (4.5)$$

Similarly to the σ meson, the equations of motion for the ω meson are similarly left unchanged, with the exception of the new constant. Here, as the cascade is a 2-strange quark particle, the constant is $w_\omega = \frac{1}{3}$, and thus we obtain the Hamiltonian for the ω part:

$$H_\omega = \frac{1}{3} G_\omega \rho_N \rho_\Xi \quad (4.6)$$

4.2.2 $\vec{b}$ Field Equation of Motion

We begin by writing the energy for the $\vec{b}$ component of the energy, which takes the form:

$$E_b = -\frac{1}{2}\int dV \left[\nabla^2 b^2 + m_\rho^2 b^2\right] + \int dV \rho_N g_b \vec{b}\cdot\frac{\vec{\tau}}{2} + \int dV \rho_\Xi g_b \vec{b}\cdot\frac{\vec{\tau}}{2} \tag{4.7}$$

However when applying the mean-field approximation, we note that only the third-component of the $\vec{\rho}$ field is non-zero, and thus we obtain:

$$E_\rho = -\frac{1}{2}\int dV \left[\nabla^2 b^2 + m_\rho^2 b^2\right] + \int dV \rho_N g_\rho b\frac{\tau_3}{2} + \int dV \rho_\Xi g_\rho b\frac{\tau_3}{2} \tag{4.8}$$

Now taking the variation with respect to the b field, we find:

$$0 = -\nabla^2 b - m_\rho^2 b + \frac{\tau_3}{2} g_\rho \left(\rho_N + \rho_\Xi\right) \tag{4.9}$$

And as before neglecting the ∇^2 term as it's contribution is small relative to the other contributions, we thus obtain:

$$g_\rho b = G_\rho \frac{\tau_3}{2}\left(\rho_N + \rho_\Xi\right) \tag{4.10}$$

Which substituting back into the energy, and ignoring the derivative term due to it's small contribution, we find the term contributing the binding energy of the Ξ hyperon in a nucleon is:

$$H_\rho = \frac{G_\rho \tau_3^N \rho_N \tau_3^\Xi \rho_\Xi}{4} \tag{4.11}$$

Now we will consider the affect of τ_3 acting on ρ_N. We note that $\rho_N = \sum_k \delta(\vec{r} - \vec{R_k})$, where we sum over the nucleons at position $\vec{R_k}$. Now if we act the third Pauli matrix on a proton, we find that the eigenvalue is $+1$, while if we act on a neutron the eigenvalue is -1, and hence:

$$\rho_3 = \sum_{proton} \delta(\vec{r} - \vec{R_p}) - \sum_{neutron} \delta(\vec{r} - \vec{R_n}) \tag{4.12}$$

And so we define this as $\rho_3 = \rho_p - \rho_n$, where ρ_p is the proton density and ρ_n is the neutron density. We will take these also to have a Woods-Saxon form when performing calculations with the proton density having the proton number Z, and the neutron density having neutron number $N = A - Z$. But this means for nuclei with $N = Z$, there is no effect from the isovector term, which is true up till ^{40}Ca.

Now the affect of the third Pauli matrix on ρ_Ξ amounts to making the contribution repulsive for Ξ^-, as the quark composition of this is dss, and thus receives a negative

contribution from the third Pauli matrix acting on the down quark. However for the Ξ^0, which has quark composition uss, this makes the contribution from isospin attractive, as the Pauli matrix give a positive contribution when acting on the up quark. Thus we can write the Hamiltonian for Ξ^0 as:

$$H_\rho = \frac{1}{4} G_\rho (\rho_p - \rho_n) \rho_\Xi \tag{4.13}$$

And for Ξ^-:

$$H_\rho = -\frac{1}{4} G_\rho (\rho_p - \rho_n) \rho_\Xi \tag{4.14}$$

Plotted in figure [4.1] is the contribution from the ρ meson in Lead, Lanthanum, and Yttrium to the binding potential for a Ξ^0 hyperon. This was done with the value for $G_\rho = 4.71$, as taken from (Martinez, Thomas, Guichon and Stone, 2020).

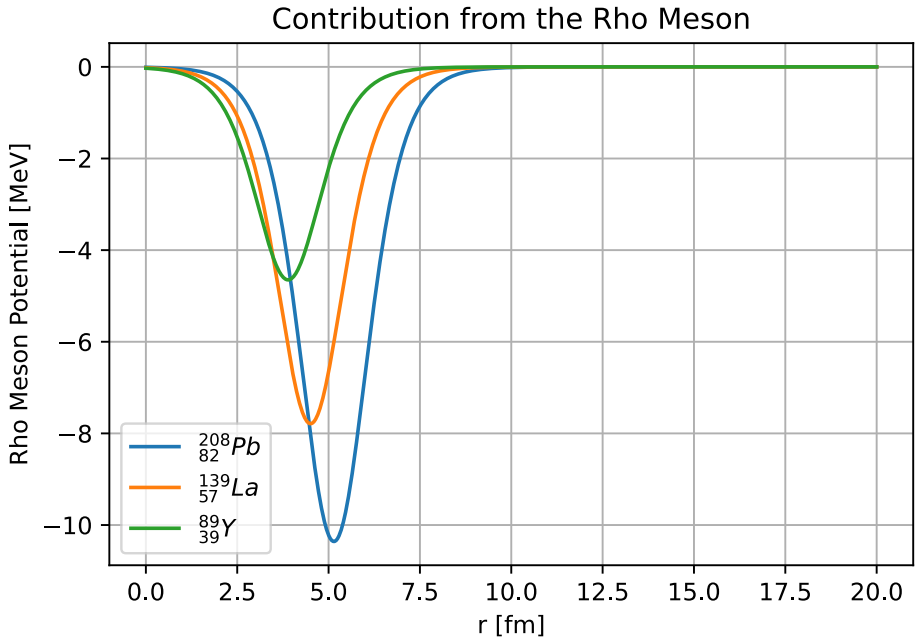

Figure 4.1: The Rho Meson Potential contribution

With the isospin contribution found, it is now possible to calculate the binding energy of the Ξ^0 hyperons.

4.3 Binding Energies of Neutral Cascades

We aim now to make a prediction for the binding energies for Ξ^0 hyperons. We make use of a similar method as to that when calculating the Λ binding energies, though now an isospin interaction must be included.

Now there is not much data for the binding energy of the cascade hyperons to fit the coupling constant for G_ρ, and thus to investigate the affect this has on the binding energy, the binding energy will be solved for $G_\rho = 4.71$ and plus minus 10% of this value. The previously calculated values of $G_\sigma = 8.65$, and $G_\omega = 5.64$ are also used here, along with the 4-body force, as this produced the results closest to experiment. The results are plotted in figure [4.2], for $G_\rho = 4.71$.

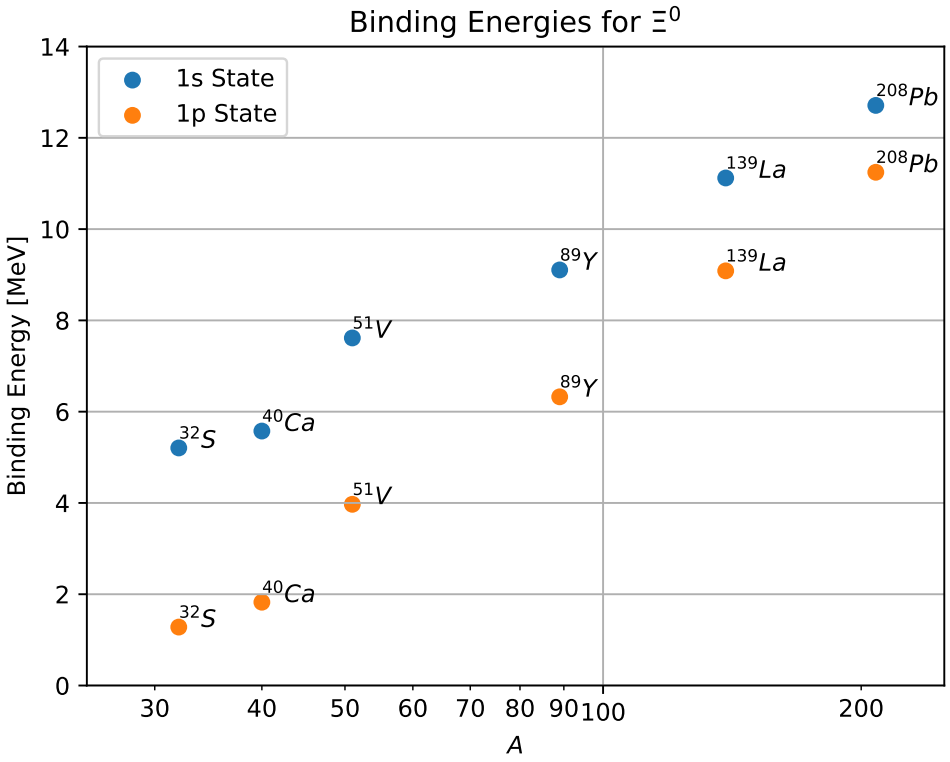

Figure 4.2: Binding Energies for $G_\rho = 4.71$

Now changing the coupling to the rho meson only affects nuclei where $N \neq Z$, and so the upper and lower bounds for the binding energy for these nuclei were also calculated. These are plotted in figure [4.3].

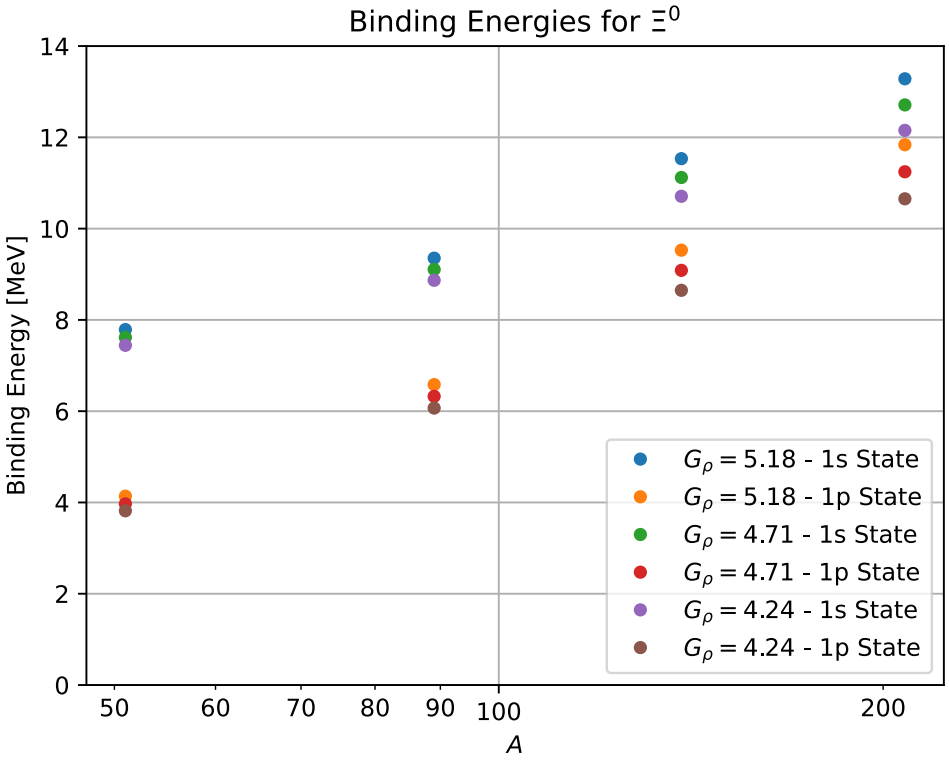

Figure 4.3: Binding Energies with the different values for G_ρ

4.4 Calculating Coulomb Potential

We will now consider adding in the effect of the Coulomb potential between the protons in the nucleus, and the Ξ^- cascade. Now the Coulomb potential is given by:

$$V(\vec{r}) = ke \int d^3r' \frac{\rho_c(\vec{r}')}{|\vec{r} - \vec{r}'|} \tag{4.15}$$

Where here k is the Coulomb constant, e is the charge of an electron, and ρ_c is the charge density of the nucleus, which takes the form:

$$\rho_c(\vec{r}) = \frac{\rho_0}{1 + \exp\left\{\left[\frac{r - R_c}{a_0}\right]\right\}} \tag{4.16}$$

Where ρ_0 is the charge density normalisation, and R_c and a_0 are parameters to fit the model.

Now, we note that the potential is a difficult integral to calculate due to the spherical nature of the charge density, which makes it difficult to deal with the $|\vec{r} - \vec{r}'|$ term. To

deal with this we note that the convolution theorem can be applied. The convolution theorem is given by:

$$\tilde{V}(\vec{q}) = (2\pi)^{3/2}\tilde{f}(\vec{q})\tilde{g}(\vec{q}) \tag{4.17}$$

Where, for our problem, we can take $g(\vec{r}-\vec{r}') = \frac{1}{|\vec{r}-\vec{r}'|}$, and $f(\vec{r}') = ke\rho_c(\vec{r}')$.

We can then find the Fourier transform of these two functions. We start by noting the Fourier transform of $g(\vec{r}-\vec{r}')$ is known, and given by:

$$\tilde{g}(\vec{q}) = \frac{4\pi}{(2\pi)^{3/2}}\frac{1}{q^2} \tag{4.18}$$

Where here $q = |\vec{q}|$. This second transform we can begin simplifying:

$$\tilde{f}(\vec{q}) = \frac{ke}{(2\pi)^{3/2}}\int d^3r' \exp\{[-i\vec{q}\cdot\vec{r}]\}r'^2\rho_c(\vec{r}') \tag{4.19}$$

Now we take our charge density to be spherically symmetric, and thus $\rho_c(\vec{r}') = \rho_c(r')$, and also take the axis of our momentum transfer $\vec{q}$ to be aligned along the z-axis, such that $\vec{r}'\cdot\vec{q} = r'q\cos(\theta)$. Thus we obtain:

$$\tilde{f}(\vec{q}) = ke\frac{2\pi}{(2\pi)^{3/2}}\int dr'r'^2\rho_c(r')\int_{-1}^{+1} d(\cos\theta)\exp\left[-iqr'\cos(\theta)\right] \tag{4.20}$$

Which evaluating the θ part gives a factor of $2j_0(qr)$, where $j_0(x)$ is the first Bessel function. Thus we find:

$$\tilde{f}(\vec{q}) = ke\frac{4\pi}{(2\pi)^{3/2}}\int dr'r'^2\rho_c(r')j_0(qr') \tag{4.21}$$

With this we can now write the Fourier transform of the Coulomb potential as:

$$\tilde{V}(\vec{q}) = ke\frac{(4\pi)^2}{(2\pi)^{3/2}}\frac{1}{q^2}\int dr'r'^2\rho_c(r')j_0(qr') \tag{4.22}$$

Then we need simply to find the inverse Fourier transform to then find the potential in space. Thus we find:

$$V(\vec{r}) = \frac{ke}{(2\pi)^{3/2}}\int d^3q \exp\{i\vec{q}\cdot\vec{r}\}\tilde{V}(\vec{q}) \tag{4.23}$$

And so substituting in $\tilde{V}(\vec{q})$:

$$V(\vec{r}) = ke\frac{2}{\pi}\int d^3q \exp\{i\vec{q}\cdot\vec{r}\}\left[\frac{1}{q^2}\int dr'r'^2\rho_c(r')j_0(qr')\right] \tag{4.24}$$

Which taking expanding the integral gives:

$$V(\vec{r}) = 4ke \int dq \int_{-1}^{+1} d(\cos(\theta) \exp\{i\vec{q} \cdot \vec{r}\} \left[\int dr' r'^2 \rho_c(r') j_0(qr') \right] \tag{4.25}$$

And aligning $\vec{r}$ along the z-axis, we find again that $\vec{r} \cdot \vec{q} = rq\cos(\theta)$, which now evaluating the θ part of the integral we find:

$$V(\vec{r}) = 8ke \int dq j_0(qr) \left[\int dr' r'^2 \rho_c(r') j_0(qr') \right] \tag{4.26}$$

Thus by evaluating this integral we find the potential in coordinate space. And we note that it is still spherically symmetric, and so can conclude:

$$V(r) = 8ke \int dq \int dr' r'^2 j_0(qr) \rho_c(r') j_0(qr') \tag{4.27}$$

This is a problem that can now be dealt with by using a simple numerical integration routine. Some examples of this finite Coulomb potential are included in figure [4.4].

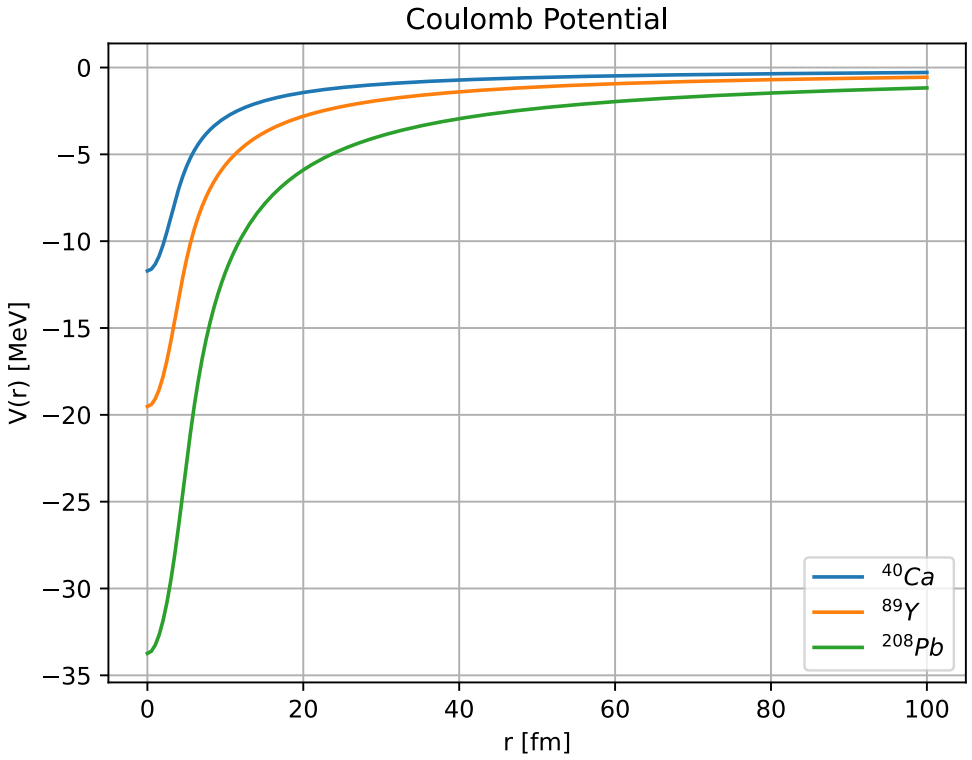

Figure 4.4: Example plots for Finite Coulomb Potentials

4.5 Binding Energies of Negative Cascades

From here it is simple to calculate the binding energies for the Ξ^- hyperons. These energies were calculated using $G_\sigma = 8.65$, $G_\omega = 5.64$, and $G_\rho = 4.71$. However, the isospin interaction is now attractive, and hence the sign for the isospin interaction is also reversed. Furthermore, it was necessary to integrate further out as the Coulomb potential goes to zero slower than the nuclear potential.

This resulted in the binding energies, plotted in figure [4.5].

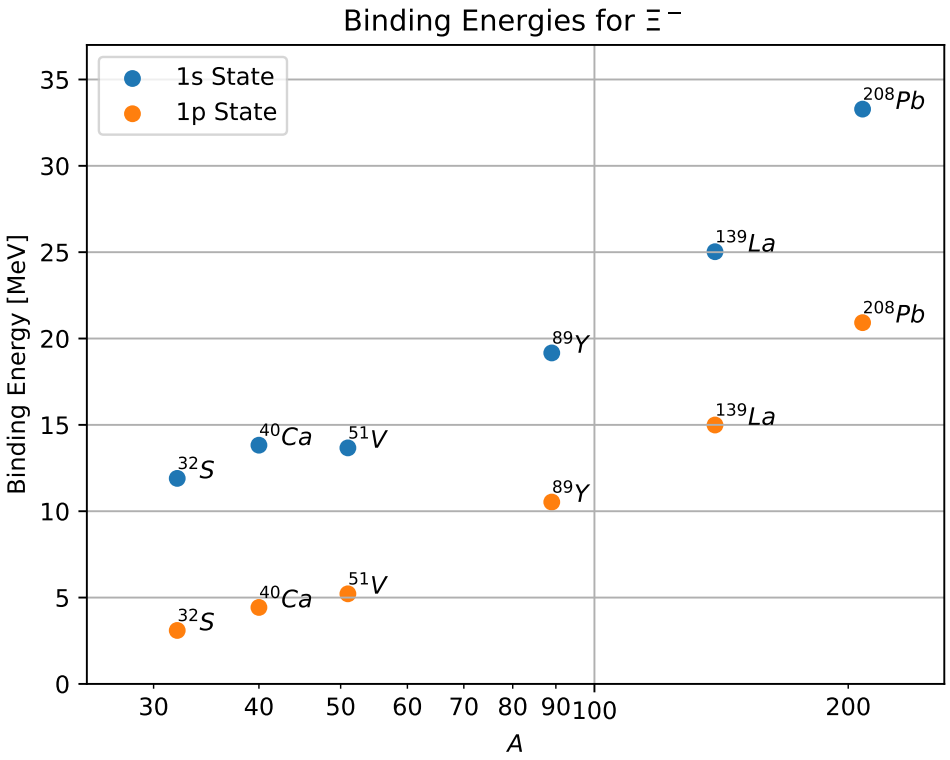

Figure 4.5: Plot of the binding energies for the negative cascade

The Coulomb potential is plotted along with the nuclear potential for $^{208}_{82}Pb$ and $^{40}_{20}Ca$ in figures [4.6a] and [4.6b]. Also included are plots with these potentials added together, in figures [4.7a] and [4.7b].

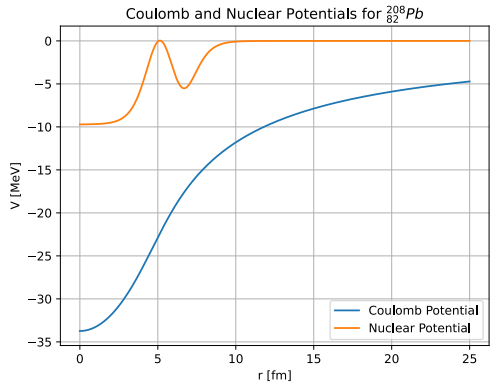

(a) Separated Binding Potentials for Ξ^- in $^{208}_{82}Pb$

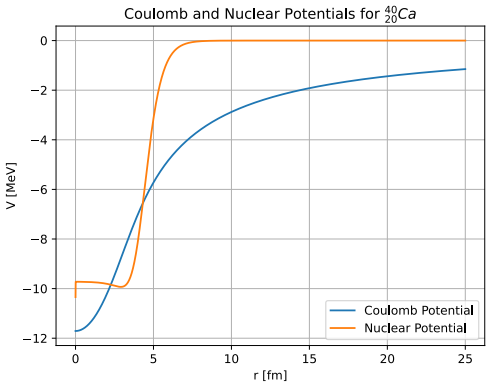

(b) Seperated Binding Potentials for Ξ^- in $^{40}_{20}Ca$

Figure 4.6: Binding Potentials for Ξ^- separated into Coulomb and Nuclear Components

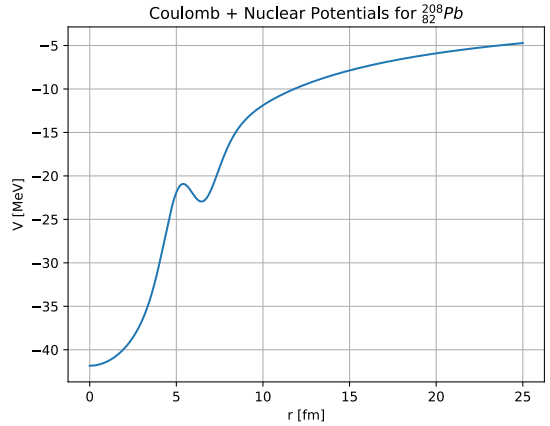

(a) Total Binding Potential for Ξ^- in $^{208}_{82}Pb$

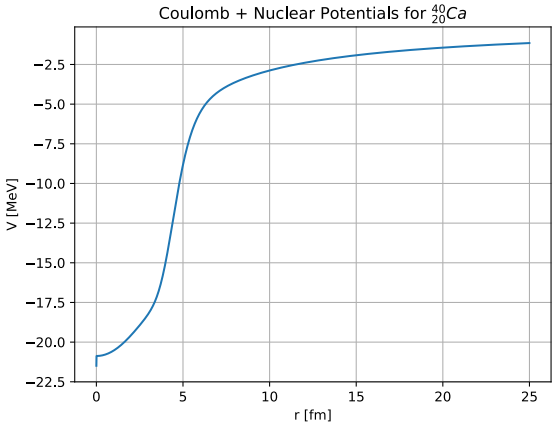

(b) Total Binding Potential for Ξ^- in $^{40}_{20}Ca$

Figure 4.7: Total Binding Potentials for Ξ^- in Lead and Calcium

Chapter 5

Cascade Coulomb Splitting

After having investigated the binding of the Ξ hyperons, we shall now turn to a more detailed investigation into how the nuclear potential contributes to the binding of the cascade into atomic states in iron and carbon atoms.

5.1 Experimental Motivation

There exists a relative abundance of experimental data for strangeness $S = -1$ systems [47], however there has yet to be much investigation into strangeness $S = -2$ systems [14] [48]. Exploring this further will help to elucidate our understanding of baryon-baryon interactions, governed by the SU(3) flavour symmetry. These systems can be Ξ hyperons, or 2 Λ or Σ systems. As there are 2 strange quarks in these systems it will also be possible to see interactions between strange quarks.

Of particular interest for this work, is that because there are now 2 strange quarks it might be important in these systems to explicitly treat quark degrees of freedom [49]. Thus, these experiments could potentially provide strong evidence in favour of a model for nuclear physics which treats quark degrees of freedom, like the QMC model.

There has in past been an experiment proposed, which will involve measuring x-rays emitted from Ξ^- hyperons bound into an atomic state in an iron atom [49]. The goal is to be able to determine the potential depth for the Ξ^--nucleus potential, by measuring the transition energy between the different energy states of the Ξ^- bound into the target. This is done by measuring the energy of the x-rays emitted during this transition. One can then compare the energy of the x-rays emitted, to the change in the energy levels for the Ξ^- calculated from the Dirac equation, with only the Coulomb potential, in order to determine the contribution from the nuclear potential. From this one could then extract the potential depth of the nuclear potential [14] [49].

Here, we shall provide a prediction using the QMC model, as to what these energy shifts should be. This shall be done by calculating the energy levels of the $5g_{9/2}$ and

$6h_{11/2}$ atomic states for a cascade bound into an iron atom. This will be done both including and excluding the nuclear potential, in order to calculate the shift in the binding energy induced by the nuclear potential. Following this a similar investigation shall be carried out for carbon, as carbon has also recently been proposed as a target to investigate Ξ^- interactions [19].

5.2 Point-like Coulomb

Now the energy transitions calculated for this experiment have previously been calculated using the Dirac equation. Furthermore, the energy transition from the $(6,5) \rightarrow (5,4)$ states is on the order of 100[keV], and so it is important to be able to find the energy accurately, to a high precision. For this reason, the Numerov algorithm no longer suffices for calculating these states. This can be shown by trying to reproduce the energy eigenvalues for the point-like Coulomb potential. These energy eigenvalues can be calculated analytically, however it was found that the values calculated using the Numerov algorithm did not converge to the analytical values.

This motivated the decision to turn to solving the Dirac equation instead, using the Runge-Kutta algorithm. It has been shown in past work to be able to reproduce the point-like hydrogen atom energy to a high precision [50]. Now to test how well the code extends to an iron atom, the point-like Coulomb potential will be tested for a number of different states. Of particular interest are the higher energy states. The point-like Coulomb potential is given by:

$$V(r) = -\alpha \frac{Z}{r} \tag{5.1}$$

Unlike the solutions to the Schrödinger equation, solutions to the Dirac equation are spinors. These take the form of:

$$\psi_\alpha(\vec{r}) = \begin{bmatrix} g_\alpha(r)\chi^\mu_\kappa(\hat{r}) \\ -if_\alpha(r)\chi^\mu_{-\kappa}(\hat{r}) \end{bmatrix} = \begin{bmatrix} \frac{G_\alpha(r)}{r}\chi^\mu_\kappa(\hat{r}) \\ \frac{-iF_\alpha(r)}{r}\chi^\mu_{-\kappa}(\hat{r}) \end{bmatrix} \tag{5.2}$$

Here, μ is a label to denote that the components containing the spin information χ have more than one component, and α is used to collectively refer to the principal quantum number and the quantum number κ, which is given by:

$$\kappa = \begin{cases} -j - \frac{1}{2} & \text{if } j = l + \frac{1}{2} \\ -j + \frac{1}{2} & \text{if } j = l - \frac{1}{2} \end{cases} \tag{5.3}$$

The wavefunction is then normalised such that:

$$\int |\psi_\alpha|^2 d^3r = \int_0^\infty r^2[\ |g_\alpha(r)|^2 + |f_\alpha(r)|^2]dr = 1 \tag{5.4}$$

State	Analytical Energy (MeV)	Numerical Energy (MeV)
$1s_{1/2}$	-23.413492	-23.413491
$2p_{3/2}$	-5.813321	-5.813321
$3d_{5/2}$	-2.580455	-2.580455
$4f_{7/2}$	-1.450869	-1.450855
$5g_{9/2}$	-0.928368	-0.928368
$6h_{11/2}$	-0.644629	-0.644623

Table 5.1: Table of Point-like Energies - Using Runge-Kutta

As the components containing the spin have the identity:

$$\int \chi_{\kappa}^{m\dagger} \chi_{\kappa'}^{m'} d\hat{r} = \delta_{\kappa\kappa'}\delta_{mm'} \tag{5.5}$$

This leads to a Dirac equation, contiaining the point Coulomb potential, of the form:

$$\frac{d}{dr}\begin{bmatrix} G_\alpha(r) \\ F_\alpha(r) \end{bmatrix} = \begin{bmatrix} -\frac{\kappa_\alpha}{r} & \lambda_\alpha + 2\mu - V_{Coulomb}(r) \\ -\lambda_\alpha + V_{Coulomb}(r) & \frac{\kappa_\alpha}{r} \end{bmatrix}\begin{bmatrix} G_\alpha(r) \\ F_\alpha(r) \end{bmatrix} \tag{5.6}$$

Where here, instead of solving directly for the energy eigenvalue, we solve for the eigenvalue $\lambda_\alpha = E_\alpha - \mu$.

Using this Dirac equation, it was shown that it was possible to recreate the required analytical energy states. The analytical solution to the energy eigenvalues are given, in natural units, by:

$$E_{n,j} \approx \mu\sqrt{1 - \frac{(Z\alpha)^2)}{\kappa^2}} - \mu \tag{5.7}$$

Where here μ is the reduced mass of the cascade and iron nucleus, and α is the fine-structure constant. Now, for the highest angular momentum states for a given energy level, κ is given by $\kappa = -n$.

The results then of the attempt at a numerical solution are compared to the analytical results in table [5.1]. As can be seen it was possible to find the energy eigenvalues to within a 10th of a keV, and so it is reasonable to assume that this solver should be appropriately accurate for the calculation of the other energy eigenvalues. And the energy of the transition between the $6h_{11/2}$ and $5g_{9/2}$ states is found to be 283.745keV.

State	Finite Energy (keV)	Point Coulomb Energy (keV)
$5g_{9/2}$	−904.504	−928.368
$6h_{11/2}$	−620.777	−644.623
$6h_{11/2}$ - $5g_{9/2}$	283.727	283.745

Table 5.2: Table of the finite Coulomb potential energies, including the transition energy

5.3 Finite Coulomb Energy Levels

Now, having validated that the solver is able to return sufficiently accurate and precise values for the point-like Coulomb potential, we can have confidence that the solver will return similarly accurate and precise values for the finite potential, as well as the nuclear potential. Using the finite Coulomb potential, as found in sec. [4.4], we shall now calculate the energy eigenvalues for a number of these states.

Now, as stated in the proposal [14], the states of interest are the $5g_{9/2}$ and the $6h_{11/2}$. Applying the finite Coulomb potential in place of the point-like Coulomb potential, we find the energies recorded in table [5.2].

And so we see that when compared to the point Coulomb potential, these have the slight effect of increasing the energy of both the $5g_{9/2}$ state and the $6h_{11/2}$ states. However, we note that the difference between the transition energies is found to be less than a 10th of a keV.

5.4 Nuclear + Finite Coulomb Energy Levels

With the finite Coulomb energy levels established, we wish now to see how the inclusion of the nuclear potential shifts the energy levels. In order to do this, we shall now have to modify the Dirac equation used. The Dirac equation with only the Coulomb potential is given by:

$$(i\gamma_\mu \partial^\mu - m - e\gamma_\mu A^\mu)\psi = 0 \tag{5.8}$$

Where A^μ is the 4-vector containing the electric and magnetic potentials. We note here that the electromagnetic potential enters in as a vector potential. Thus, the ω and ρ mesons will enter into the Dirac equation in a similar manner then, as they are vector mesons. The σ meson however will enter into the equation like the mass term, as the σ meson is a scalar meson. So, we find then, a Dirac equation of the form:

$$\left[i\gamma_\mu(\partial^\mu - eA^\mu + g_{\omega\Xi}\omega^\mu + g_{\rho\Xi}\rho^\mu_\alpha \frac{\tau_\alpha}{2}) - (m - g_{\sigma\Xi}\sigma)\right]\psi \tag{5.9}$$

Where here the coupling constants are coupling the meson fields to the cascade, and thus we have $g_{\sigma\Xi} = wg_\sigma$, $g_{\omega\Xi} = \frac{1}{3}g_\omega$ and $g_{\rho\Xi} = g_\rho$ [41]. Then, as the solutions found were in the mean-field approximation, we note that $\omega^{i=1,2,3}(r) = 0$ and all components of the ρ meson except for $\rho_3^0(r) = b_3(r)$ are zero. And finally, there is no magnetic potential considered here, and so we find the Dirac equation:

$$\left[i\gamma_\mu\partial^\mu + i\gamma_0(-eA^0(r) + \frac{1}{3}g_\omega\omega^0(r) + g_\rho b_3(r)\frac{\tau_3}{2}) - (m - wg_\sigma(r)\sigma)\right]\psi \tag{5.10}$$

$$V(r) = V_{Coulomb}(r) + \frac{1}{3}g_\omega\omega(r) + g_\rho b_3(r)\frac{\tau_3}{2} \tag{5.11}$$

Thus, we obtain the new equation:

$$\frac{d}{dr}\begin{bmatrix} G_\alpha(r) \\ F_\alpha(r) \end{bmatrix} = \begin{bmatrix} -\frac{\kappa_\alpha}{r} & \lambda_\alpha + 2\mu - wg_\sigma\sigma(r) - V(r) \\ -\lambda_\alpha + wg_\sigma\sigma(r) + V(r) & \frac{\kappa_\alpha}{r} \end{bmatrix}\begin{bmatrix} G_\alpha(r) \\ F_\alpha(r) \end{bmatrix} \tag{5.12}$$

Now, from earlier, we saw that the solutions to these meson fields are given by:

$$g_\sigma\sigma = -\frac{1}{m_\sigma^2}\vec{\nabla}^2\left[G_\sigma\rho_N + wG_\sigma\rho_\Xi\right] + G_\sigma\rho_N(1 - d[G_\sigma\rho_N + wG_\sigma\rho_\Xi]) + G_\sigma\rho_\Xi(w - \tilde{w}d[G_\sigma\rho_N + wG_\sigma\rho_\Xi])\left[1 - \frac{P_\Xi^2}{2M_\Xi^2}\right] \tag{5.13}$$

$$g_\omega\omega = -\frac{1}{m_\omega^2}\vec{\nabla}^2\left[G_\omega\rho_N + wG_\omega\rho_\Xi\right] + G_\omega\rho_N + w_\omega G_\omega\rho_\Xi \tag{5.14}$$

$$g_\rho b(r) = G_\rho\frac{\tau_3}{2}\left(\rho_N + \rho_\Xi\right) \tag{5.15}$$

Now, when substituting into the Dirac equation, we neglect the terms which contain any factors of ρ_Ξ, as these terms would correspond to the interactions between more than one cascade hyperon. However, we recognise then that there is no 4-body interaction, to which the coupling constants were fitted. Here, as there are no Ξ density terms, we note that this expansion goes as the original many-body expansion [8]. Thus we can take the σ meson field as:

$$g_\sigma\sigma = -\frac{1}{m_\sigma^2}\vec{\nabla}^2\left[G_\sigma\rho_N\right] + G_\sigma\rho_N(1 - dG_\sigma\rho_N + d^2G_\sigma^2\rho_N^2) \tag{5.16}$$

Which we seen now includes a final term which will correspond to a 4-body interaction. Using these, the energies were calculated and recorded in table [5.3].

As can be seen from this, the introduction of the nuclear potential causes a greater shift in the energy of the $5g_{9/2}$ state, than in the $6h_{11/2}$ state. This leads to the transition energies shifting by about 2.898keV, as can be seen in table [5.4].

State	Energy (keV)
$5g_{9/2}$	-907.425
$6h_{11/2}$	-620.800
$6h_{11/2}$ - $5g_{9/2}$	286.625

Table 5.3: Table energies now including the nuclear potential, and the transition energy

State	Nuclear Potential (keV)	Finite Coulomb (keV)	Energy Shift (keV)
$5g_{9/2}$	-907.649	-904.504	3.145
$6h_{11/2}$	-620.800	-620.777	0.023
$6h_{11/2}$ - $5g_{9/2}$	286.849	283.727	3.122

Table 5.4: Table comparing the energies after including the nuclear potential, as well as the finite Coulomb potential

5.5 Alternative Approach to Nuclear Potential

Now, we shall also consider an alternative approach to including the nuclear potential. This is to make an approximation which does not distinguish between the Lorentz scalar and vector potentials. This makes it comparable to the Hamiltonians used in ch. [4]. From here, we shall introduce a term to the Hamiltonian corresponding to a Dirac equation. Then taking the variation with respect to $\psi^{\dagger}_{\Xi}$, it is possible to find an equation of motion for ψ_{Ξ}. This process amounts to essentially solving the Dirac equation, of the form:

$$\frac{d}{dr}\begin{bmatrix} G_\alpha(r) \\ F_\alpha(r) \end{bmatrix} = \begin{bmatrix} -\frac{\kappa_\alpha}{r} & \lambda_\alpha + 2\mu - V_C(r) - V_{Binding}(r) \\ -\lambda_\alpha + V_C(r) + V_{Binding}(r) & \frac{\kappa_\alpha}{r} \end{bmatrix}\begin{bmatrix} G_\alpha(r) \\ F_\alpha(r) \end{bmatrix} \tag{5.17}$$

Where here, the potential, $V_{Binding}$ is the same as has been used in the previous chapters, as in equation [3.19], though here it is the equivalent for a cascade hyperon. A table summarising the energies calculated using this method are included in table [5.5].

As can be seen, the difference between these two methods is small, amounting into a difference in the transition energy of 0.303keV.

State	First Method (keV)	Alternative Method (keV)	Difference (keV)
$5g_{9/2}$	−907.649	−907.153	0.496
$6h_{11/2}$	−620.780	−620.799	0.001
$6h_{11/2}$ - $5g_{9/2}$	286.625	286.332	0.303

Table 5.5: Table comparing the energies of the two different methods for including the nuclear potential

State	Analytical Energy (keV)	Numerical Energy (keV)
$2p_{3/2}$	−144.3036	−144.3036
$3d_{5/2}$	−64.1307	−64.1307
$4f_{7/2}$	−36.0727	−36.0726

Table 5.6: Table of Point-like Energies - Carbon Atoms

5.6 Carbon Atomic Energies

We shall now consider the atomic binding of the negative cascade hyperon into a carbon atom, as carbon has been considered as a possible alternative target. It has been proposed to look at the transitions $(4,3) \to (3,2)$ and $(3,2) \to (2,1)$, as these transitions have been shown to have transitions in the order of 100keV, and also to show a reasonable amount of energy shift, due to the nuclear interaction.

Once again, we shall verify that the solver implemented provides sufficient precision and accuracy, by testing the point Coulomb potential energies. The results of this are recorded in table [5.6]. As can be seen it is possible to reproduce the energy for these state, to within a 10th of a keV once again.

Hence, we turn to calculating the finite Coulomb potential. In past it has been shown that the charge density for carbon can be fit to a Woods-Saxon density, using slightly adjusted parameters [51]. Here, we take the parameters, $\rho_0 = 0.15[\text{fm}^{-1}]$, $c = 1.1[\text{fm}]$, and $a = 0.65[\text{fm}]$.

With these parameters, the finite Coulomb energies were calculated, and recorded in table [5.7].

Finally, we consider adding in the nuclear potential. We shall do this by using the modified Dirac equation, once again with 4-body interactions present. The energies are recorded in table [5.8].

We see then that this results in a shift in the energy transitions of 5.379keV for the $(3,2) \to (2,1)$ transition.

State	Energy (keV)
$2p_{3/2}$	-0.138724
$3d_{5/2}$	-0.058433
$4f_{7/2}$	-0.030575

Table 5.7: Table of Finite Coulomb Energies - Carbon Atoms

State	Nuclear Potential (keV)	Finite Coulomb (keV)	Energy Shift (keV)
$2p_{3/2}$	-143.792	-138.724	5.068
$3d_{5/2}$	-58.621	-58.433	0.188
$4f_{7/2}$	-30.575	-30.575	0.000
$3d_{5/2}$ - $2p_{3/2}$	85.170	80.291	4.880
$4f_{7/2}$ - $3d_{5/2}$	28.046	27.858	0.188

Table 5.8: Table comparing the energies with and without the nuclear potential- Carbon

Chapter 6

Neutral Sigma Hyperon Calculations

The final hyperon to be investigated is the Σ^0 hyperon. Here we aim not to calculate the binding energy but rather to calculate the expectation value of the σ meson field in nuclear matter. This will then be used to calculate the magnetic moment of the Σ^0 in the nuclear environment in order to produce an experimental prediction.

6.1 Experimental Motivation

An interesting phenomena which is predicted by the QMC model approach, is that the magnetic moment of the Σ^0 hyperon is different in free space, when compared to when it is bound in nuclear matter [52]. One can show then that the interaction with the σ meson field leads to the spreading out of the up and down quark wavefunctions [53], which corresponds then to a change in the magnetic moment.

However, it is not possible to measure this change in the magnetic moment directly. Instead, one must investigate the decay:

$$\Sigma^0 \rightarrow \Lambda^0 + \gamma \tag{6.1}$$

Where on the left the spins of the up and down quarks are aligned such that they have a total spin of 1. The decay conserves spin then by emitting a photon, while the spin of the up and down quarks in the Lambda become anti-aligned. This is known as a magnetic transition, and here the decay rate is proportional to the magnetic moment of the light quark.

To provide a prediction for the change in the magnetic moment, one must first obtain the σ meson expectation value, in the nuclear environment. This can then be used to calculate the magnetic moment for the Σ hyperon in the nuclear environment.

6.2 Finding the Wavefunction

It is of interest to consider the binding of the Σ^0 into a Helium nucleus. However, when dealing with this nucleus, it is no longer appropriate to use a Woods-Saxon density. Instead the density used takes the form:

$$\rho(r) = \frac{\rho_0}{1 + \exp\left[(r-c)/1\right]}\left(1 + w\frac{r^2}{c^2}\right) \tag{6.2}$$

Then, it is important to normalise the density. The binding shall be into ^4He, and thus we require:

$$\int dV \rho(r) = 4 \tag{6.3}$$

As there are 4 nucleons in this Helium nucleus. The parameters taken are $c = 0.964$[fm], $a = 0.322$[fm], and $w = 1.74$ [54]. The normalised density is plotted in figure [6.1], for those parameters. With this the equations of motion for the meson fields remain the same, with the exception of the different form for the density.

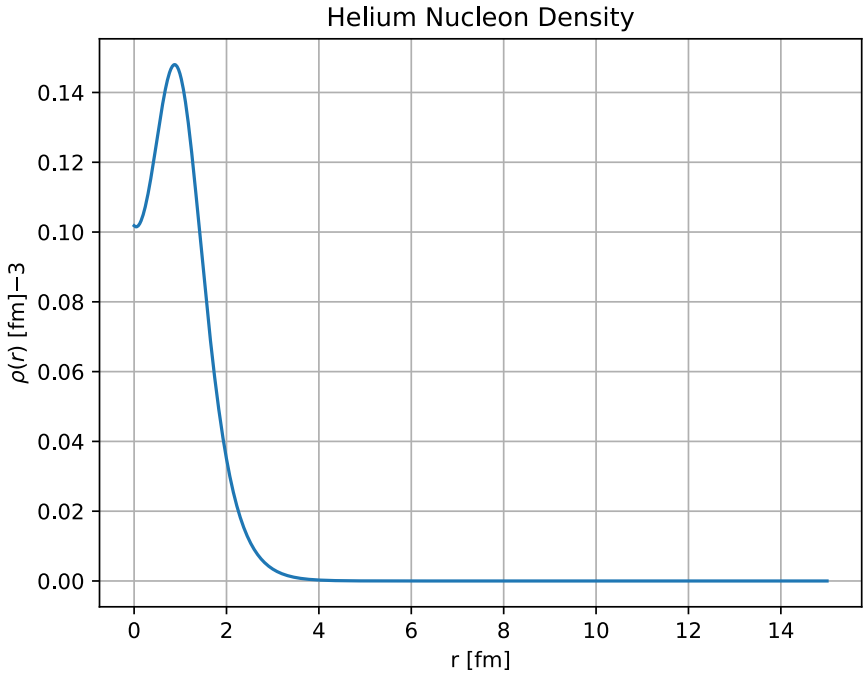

Figure 6.1: Plot of Density for Helium nucleus (Normalised)

Now the binding energy of a Σ^0 hyperon into a Helium nucleus is known to be 7.6[MeV]. Furthermore, we note that the isospin is zero for a Helium nucleus, as $N = Z$,

and the Σ^0 is an electrically neutral hyperon, and thus there is no isovector nuclear force, or Coulomb potential to account for. This leaves just interactions with the sigma and omega meson fields. As we are interested in the sigma field, the omega coupling will be adjusted to fit to the binding energy. Once this has been completed, then the wavefunction can be found for this given energy and set of coupling constants. Here we are exploring Helium binding, and so it is impractical to consider a 4-body force, due to the number of nucleons present, and so for this calculation, only the 2 and 3 body forces are considered. Included is a plot of $r^2\psi^2$, in figure [6.2], with $G_\sigma = 8.65$, which corresponds to a value for $G_\omega = 3.69$. The potential is also plotted in figure [6.3]

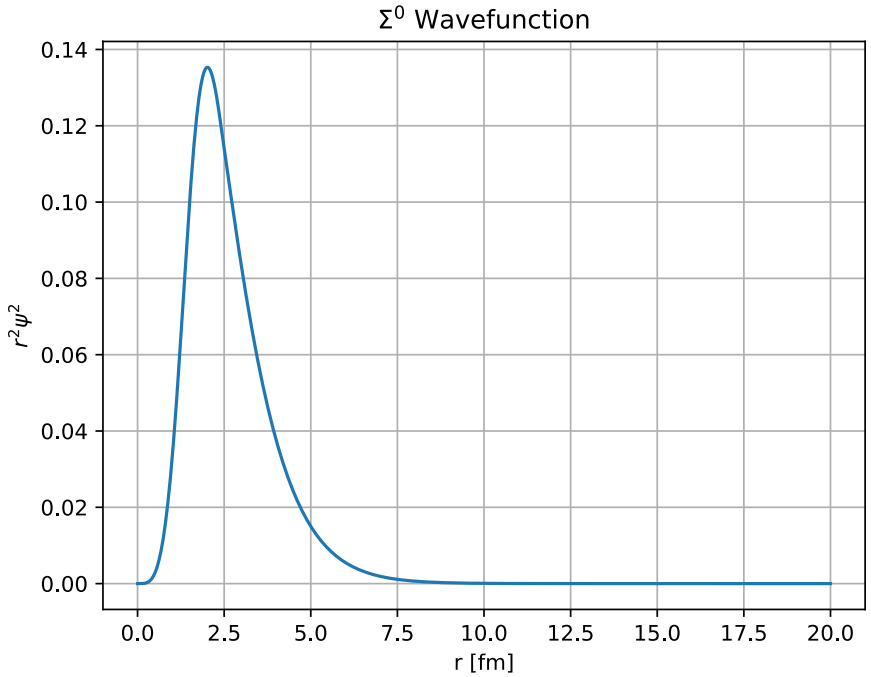

Figure 6.2: Plot of $r^2\psi^2$

6.3 Calculating the Mean Field

Now we turn to calculating the mean sigma meson field, and the mean density. These are given by:

$$\langle g_\sigma \sigma \rangle = \int dV g_\sigma \sigma(r) \left|\Psi_{\Sigma^0}(\vec{r})\right|^2 \tag{6.4}$$

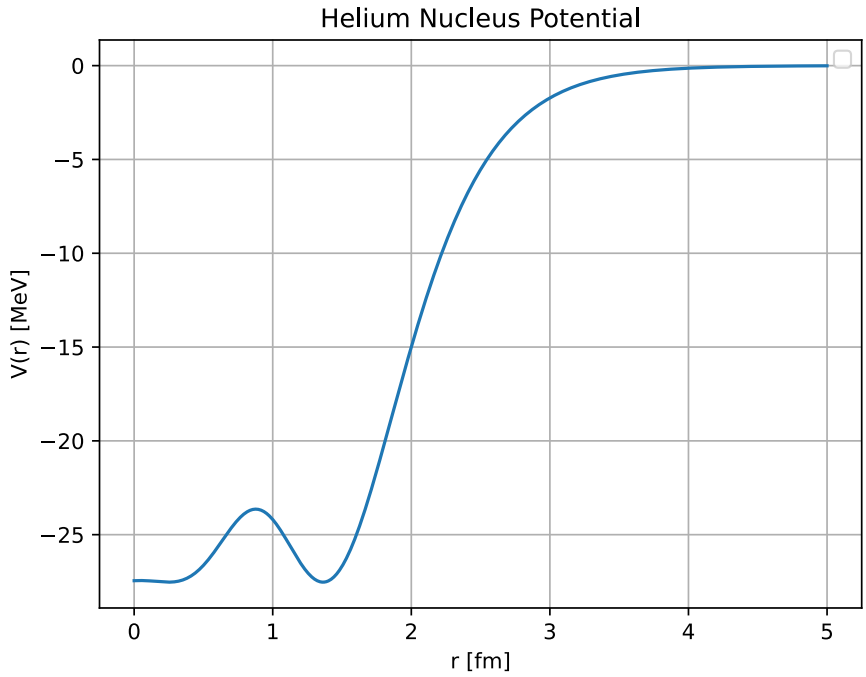

Figure 6.3: Binding Potential for a Σ^0 Hyperon

$$\langle \rho \rangle = \int dV \rho(r) \left| \Psi_{\Sigma^0}(\vec{r}) \right|^2 \tag{6.5}$$

Now the equation for the sigma field is obtained from the equations of motion, and is given by:

$$g_\sigma \sigma = G_\sigma \rho_N (1 - d G_\sigma \rho_N) \tag{6.6}$$

Now the Numerov solver outputs $u(r) = r\psi(r)$, not $\psi(r)$, however this can be sidestepped as a problem when including this factor of r, with that which arises from the volume element in the total integral. Thus upon expanding the volume element, we can simplify this to:

$$\langle g_\sigma \sigma \rangle = 4\pi \int dr \; g_\sigma \sigma(r) \left| u_{\Sigma^0}(r) \right|^2 \tag{6.7}$$

$$\langle \rho \rangle = 4\pi \int dr \; \rho(r) \left| u_{\Sigma^0}(r) \right|^2 \tag{6.8}$$

And when evaluating these for $G_\sigma = 8.65$, we find $\langle g_\sigma \sigma \rangle = 103.23[\text{MeV}]$ and $\langle \rho \rangle = 0.07258[\text{fm}]^{-3}$.

However it is of interest to find this in terms of the quark coupling, and not the nucleon coupling. Thus, we are interested in finding $< g_\sigma^q \sigma >$. As in sec. [2.2.1], we saw that the relation between the quark and nucleon coupling was:

$$g_\sigma = 3 g_\sigma^q S(\sigma = 0) \tag{6.9}$$

And hence, so, we can find the expectation value of $< g_\sigma^q \sigma >$, by:

$$< g_\sigma^q \sigma >= \frac{g_\sigma^q}{g_\sigma} < g_\sigma \sigma > \tag{6.10}$$

And so now, we must evaluate $S(\sigma = 0)$. It is a good approximation to take $\Omega_0 \approx 2.04$ as the eigenfrequency, and $m_q = 0$. With these, we find the expression for $S(\Sigma = 0)$ simplifies to:

$$S(\sigma = 0) = \frac{1/2}{(\Omega_0 - 1)} \tag{6.11}$$

$$S(\sigma = 0) = \frac{1/2}{1.04} = 0.4808 \tag{6.12}$$

Next we can find the the nucleon coupling by taking:

$$g_\sigma = m_\sigma \sqrt{G_\sigma} \tag{6.13}$$

Here we shall take $m_\sigma = 504$[MeV], which gives the nucleon coupling $g_\sigma = 7.512$, after taking into account that g_σ should be unitless, and thus the quark coupling is given as, $g_\sigma^q = 5.209$. This leads to the expectation value of the sigma meson field, coupled to the quark is given as $< g_\sigma^q \sigma >= 71.57$[MeV].

Conclusions

It is fitting at this point to summarise the findings of this work. In this work, a many-body expansion of the QMC model involving hyperons has been accomplished, done in the same vein of the work completed by Guichon & Thomas [8].

This expansion was first applied to Lambda hyperons. In this first case, the isospin-dependent contribution was ignored, as the Lambda has zero isospin. In addition, the spin-orbit interaction was taken to be zero as well, as this is small for Lambda hyperons. With this, it was possible to fit the coupling constants of the σ and ω meson fields. This was carried out using experimental values for the binding energy of the 1s and 1p states for Lambda hyperons ranging from A=32, up to A=208. It is of interest to note that including terms up to 4-body interactions returned the best fit, with the 3-body fit being the worst. Thus, throughout the rest of the work the 4-body interactions were included. The results of these fits can be found in figures [3.3a]-[3.3c].

Using these coupling constants it was possible to extend the model to calculate the binding energy of the cascade hyperons. To do this the isospin-dependent interaction was introduced, as well as the finite Coulomb potential. It is worth noting that the coupling to the rho meson was not fitted, so a few different values were investigated to see how changing this coupling would affect the binding energy. The predictions for these binding energies can be found in figures [4.2], [4.3] and [4.5].

Following this an investigation into the atomic binding energy of the negative cascade in carbon and iron nuclei was carried out. Of particular interest was calculating the shift in the atomic energy levels due to the strong interaction, as this effect is to be investigated at J-PARC. So, to carry this out, the energy eigenvalues for the relevant energy eigenstates were calculated, both including and excluding the nuclear potential. It was found that the energy shift due to the nuclear potential in iron, for the transition between the $5g$ and $6h$ states, was 3.122[keV]. In carbon for the $2p$ and $3d$ states the shift in the transition energy was 4.880[keV].

Finally, the mean value of the sigma meson field and the mean nucleon density was calculated for the Sigma hyperon, bound in Helium. Here the coupling constant for the omega meson was refit, to match the binding energy of the Sigma hyperon in Helium. Then using this, the corresponding wavefunction could be found, and then these values could be calculated. It was found that $< g_\sigma^q \sigma >= 71.57$[MeV], and $< \rho_N >= 0.07258$[fm^{-3}]. The mean value of the sigma field will be used now to calculate a prediction for the change in the magnetic moment of the Sigma hyperon in and out of the nuclear medium.

Appendix A

Numerical Details of the Numerov Algorithm

Throughout this work, to solve the eigenvalue problem above, the Numerov algorithm will be employed. The advantage of using this algorithm is that it can be employed for any given value of energy, and will provide a way to test for whether the solution for that given energy is a valid eigenvalue, as will be seen in [A.2].

A.1 Numerov Algorithm Details

Numerov's algorithim is equipped to solve differential equations of the form:

$$\frac{d^2y}{dx^2} = f(y, x) \tag{A.1}$$

Which is the form for which we have arranged our problem here. The Numerov algorithm works in an iterative manner, by using the past two points to determine what the next should be [55]. This is derived from making the Taylor expansion of $y(x)$ around a small step h, which gives:

$$y(x \pm h) = y(x) \pm hy'(x) + \frac{h^2}{2}y''(x) \pm \frac{h^3}{6}y'''(x) + \frac{h^4}{24}y^{(iv)}(x) \tag{A.2}$$

One can then use this to derive the identity:

$$\frac{y(x+h) + y(x-h) - 2y(x)}{h^2} = y''(x) + \frac{h^2}{12}y^{(iv)}(x) \tag{A.3}$$

$$\equiv \left(1 + \frac{h^2}{12}\frac{d^2}{dx^2}\right) y''(x) \tag{A.4}$$

Now, the left hand term can be identified as the central-difference for the second derivative of $y(x)$. Making use of this, and the identity, upon rearranging, and taking note of the fact that in our situation, the right hand side is a function of x only, one can arrive at an expression:

$$y(x+h) = \left\{2\left[1 - \frac{5h^2}{12}f(x)\right]y(x) - \left[1 + \frac{h^2}{12}f(x-h)\right]y(x-h)\right\} \Big/ \left[1 + \frac{h^2}{12}f(x+h)\right] \tag{A.5}$$

Thus, provided that one knows the function $f(x)$, for all points, one has a method of finding $y(x+h)$ if they know points $y(x)$ and $y(x-h)$, which provides a way to iterate to solve for $y(x)$.

A.2 Solving the Eigenvalue problem with the Numerov Algorithm

With the details of the Numerov algorithm established, we shall now consider how to apply the algorithm to solve the problem at hand. The wavefunction for the Λ hyperon, bound into a nucleus, should be qualitatively similar to that of the hydrogen atom. Thus, as $u(r) = r\psi$, we expect that $u(0) = 0$, and as $r \to \infty$, $u(r) \to 0$. Furthermore the wavefunction should be continuous and smooth at all points. Now to ensure the first three conditions, the solution will be split into a left and right side solution, $u_L(r)$ and $u_R(r)$ respectively, where the solutions integrate inwards to a match point r_{match}. This enables us to implement the boundary conditions by taking $u_L(0) = 0$, and $u(r_{end}) = \delta$, where r_{end} is the endpoint for the solution we find, and δ is small. Then, continuity can be enforced by matching the solutions at the match point, as below:

$$u_L(r) \to u_L(r) \times \frac{u_R(r_{match})}{u_L(r_{match})} \tag{A.6}$$

At this point it is worth noting that the value chosen for δ is actually not important, as this will only change the scale of the right hand side solution, which after matching the solutions, and then normalising the solution becomes unimportant. It is only important to ensure that the value for r_{end} is sufficiently far out so as to be approaching zero, so that a valid solution is determined.

Thus, three of the four required conditions are satisfied for any given energy eigenvalue. This provides a way to test for whether an energy eigenvalue has been found, by testing whether the wavefunction is smooth or not. This condition is given by:

$$\left.\frac{\partial u_R}{\partial r}\right|_{r_{match}} = \left.\frac{\partial u_L}{\partial r}\right|_{r_{match}} \tag{A.7}$$

To do this we take an approximation for the first derivatives of these functions around the match point:

$$\left.\frac{\partial u_L}{\partial r}\right|_{r_{match}} \approx \frac{u_L(r_{match}) - u_L(r_{match-1})}{h} \tag{A.8}$$

$$\left.\frac{\partial u_R}{\partial r}\right|_{r_{match}} \approx \frac{u_R(r_{match+1}) - u_R(r_{match})}{h} \tag{A.9}$$

And then by selecting a given tolerance, ϵ, we can test if the solution is sufficiently smooth:

$$\left|\frac{u_L(r_{match}) - u_L(r_{match-1})}{h} - \frac{u_R(r_{match+1}) - u_R(r_{match})}{h}\right| < \epsilon \tag{A.10}$$

Which simplifies upon combining u_R and u_L, into one function $u(r)$:

$$\left|\frac{u_{match+1} + u_{match-1} - 2u_{match}}{h}\right| < \epsilon \tag{A.11}$$

Should this hold, then a valid solution to the eigenvalue has been found[1].

An example solution to the binding energy of ^{208}Pb is plotted in figure [A.1], for a chosen set of coupling constants.

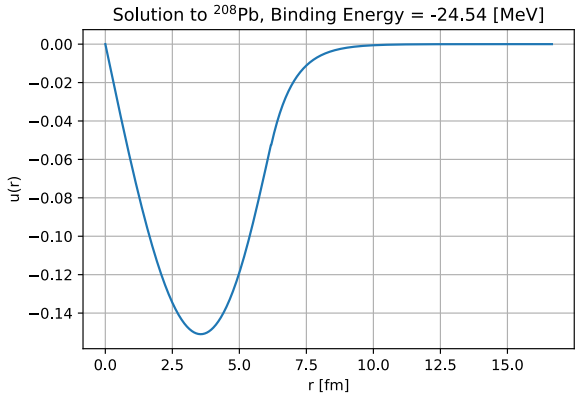

Figure A.1: $u(r)$ for ^{208}Pb, with $G_\sigma = 8.65$, $G_\omega = 5.60$

[1]The implementation of this, as well as all the other code in this project can be found at: github.com/NathanaelBotten/MPhil-Code.

Bibliography

[1] W Williams. *Nuclear and Particle Physics*. Clarendon Press, 1991.

[2] N Glendenning. *Compact Stars: nuclear physics, particle physics and general relativity*. Springer, 1997.

[3] S Wong. *Introductory Nuclear Physics*. Prentice Hall, 1990.

[4] P Guichon, K Saito, E Rodionov, and A Thomas. The role of nucleon structure in finite nuclei. *Nuclear Physics A*, 601, 1996.

[5] A Obertelli and H Sagawa. *Modern Nuclear Physics*. Springer, Singapore, 2021.

[6] B Serot and J Walecka. Properties of finite nuclei in a relativistic quantum field theory. *Physical Letters B*, 1979.

[7] B Serot and J Walecka. Relativistic nuclear many-body theory. *Recent Progress in Many-Body Theories*, 1992.

[8] P Guichon and A Thomas. Quark structure and nuclear effective forces. *Physical Review Letters*, 93, 2004.

[9] T Skyrme. The effective nuclear potential. *Nuclear Physics*, 1959.

[10] D Vautherin and D Brink. Hartree-fock calculations with skyrme's interaction. i. spherical nuclei. *Physical Review C*, 1972.

[11] O Hashimoto and H Tamura. Spectroscopy of Λ hypernuclei. *Progress in Particle and Nuclear Physics*, 2006.

[12] D Millener, C Dover, and A Gal. Λ-nucleus single-particle potentials. *Physical Review C*, 1988.

[13] E Friedman and A Gal. Constraints from Λ hypernuclei on the ΛNN content of the Λ-nucleus potential and the 'hyperon puzzle'. *Physics Letters B*, 2023.

[14] M Fujita, R Honda, L Hosomi, Y Ishikawa, H Kanauchi, T Kokie, H Tamura, M Ukai, and T Yamamoto. The Ξ atom x-ray spectroscopy at J−Parc. In *Proceedings of the 8th International Conference on Quarks and Nuclear Physics*, 2019.

[15] P Guichon, A Thomas, and K Tsushima. Binding of hypernuclei in the latest quark-meson coupling model. *Nuclear Physics A*, 2008.

[16] R Shyam, K Tsushima, and A Thomas. Production of cascade hypernuclei via the (K^-, L^+) reaction within a quark-meson coupling model. *Nuclear Physics A*, 2012.

[17] K Tsushima, K Saito, J Haidenbauer, and A Thomas. The quark-meson coupling model for Λ, Σ and Ξ hypernuclei. *Nuclear Physics A*, 1998.

[18] O Takeshi, O Yamamoto, M Fujita, T Gogami, T Harada, S Hayakawa, K Hosomi, Y Ichikawa, Y Ishikawa, K Kamada, H Kanauchi, T Koike, K Miwa, T Nagae, T Oura, Fa nd Takahashi, H Tamura, K Tanida, M Ukai, and E03/E07/E96 Collaborations. X ray spectroscopy on Ξ^- atoms (J−PARC E_{03}, E_{07} and future). In *EPJ Web of Conferences*, 2022.

[19] T Yamamoto, M Fujita, K Tanida, Y Ishikawa, K Kamada, T Koike, F Oura, H Tamura, and M Ukai. Measurement of X rays from Ξ^- C atom with an active fiber target system. Technical report, J-Parc, 2022.

[20] T Nagae, T Miyachi, T Fukuda, H Outa, T Tamagawa, J Nakano, R Hayano, H Tamura, Y Shimizu, K Kubota, R Chrien, R Sutter, A Rusek, W Briscoe, R Sawafta, E Hungerford, A Empl, W Naing, C Neerman, K Johnston, and M Planinic. Observation of a ${}^{4}_{\Sigma}$He bound state in the ^{4}He(K^-, π^-) reaction at 600 MeV/c. *Physical Review Letters*, 1998.

[21] A Borissov and S Solokhin. Production of the Σ^0 hyperon and search of Σ^0 hypernuclei at LHC with ALICE. *Physics of Atomic Nuclei*, 2022.

[22] D Griffiths. *Introduction to Elementary Particles*. Wiley-VCH, 2nd edition, 2008.

[23] M Peskin and D Schroeder. *An Introduction to Quantum Field Theory*. Westview Press, 1995.

[24] G Zweig. An SU_3 model for strong interaction symmetry and its breaking. *CERN - Developments in the Quark Theory of Hadrons*, 1964.

[25] M Gell-Mann. Nonleptonic weak decays and the eightfold way. *Physical Review Letters*, 1964.

[26] M Gell-Mann. A schematic model of baryons and mesons. *Physics Letters*, 1964.

[27] H Fritzsch, M Gell-Mann, and H Leutwyler. Advantages of the color octet gluon picture. *Physics Letters*, 1973.

[28] P Langacker. *The Standard Model and Beyond*. CRC Press, 2010.

[29] I Aitchison and A Hey. *Gauge Theories in Particle Physics - Volume II*. Institute of Physics Publishing, 2004.

[30] A Thomas. Role of quarks in nuclear structure, 2020.

[31] H Nemura and T Ishii, N andHatsuda. Hyperon-nucleon force from lattice QCD. *Physics Letters B*, 2009.

[32] S Beane, E Change, S Cohen, W Detmold, H Lin, K Orginos, Parreno, M Savage, and B Tiburzi. Magnetic moments of light nuclei from lattice quantum chromodynamics. *Physical Review Letters*, 2014.

[33] S Weinberg. On the development of effective field theory. *The European Physical Journal H*, 2021.

[34] J Iizuka. A systematics and phenomenology of meson family. *Supplement of the Progress of Theoretical Physics*, 1966.

[35] K Martinez, A Thomas, P Guichon, and J Stone. Tensor and pairing interactions within the quark-meson coupling energy-density functional. *Physical Review C*, 2020.

[36] A Chodos, R Jaffe, K Johnson, and C Thorn. Baryon structure in the bag theory. *Physical review D*, 10, 1974.

[37] A Chodos, R Jaffe, C Thorn, and V Weisskopf. New extended model of hadrons. *Physical Review D*, 1974.

[38] D Halliday. *Introductory Nuclear Physics*. John Wiley & Sons, 1955.

[39] G Eder. *Nuclear Forces*. The M.I.T Press, 1968.

[40] W Brückner, M Faessler, T Ketel, K Kilian, J Niewisch, B Pietrzyk, B Povh, H Ritter, M Uhrmacher, P Birien, H Catz, A Chaumeaux, J Durand, B Mayer, J Thirion, R Bertini, and O Bing. Spin-orbit interaction of lambda particles in nuclei. *Physics Letters B*, 1978.

[41] J. R. Stone, A. W. Thomas, and PAM Guichon. Quark–Meson-Coupling (QMC) model for finite nuclei, nuclear matter and beyond. *Progress in particle and nuclear physics*, 100, 2018.

[42] K Tsushima, K Saito, and A Thomas. Self-consistent description of Λ hypernuclei in the quark-meson coupling model. *Physics Letters B*, 1997.

[43] A Gal, E Hungerford, and D Millener. Strangeness in nuclear physics. *Reviews of Modern Physics*, 2016.

[44] S Pal, R Ghosh, B Chakrabarti, and A Bhattacharya. A study on binding energies of Λ hypernuclei. *The European Physics Journal Plus*, 2017.

[45] D Blatt and B McKellar. Four-body forces in nuclear matter. *Physical Review C*, 1975.

[46] G Brown, A Green, W Gerace, and E Nyman. Four-body forces in nuclear matter. *Nuclear Physics A*, 1968.

[47] C Dover and A Gal. Ξ hypernuclei. *Annals of Physics*, 1983.

[48] T Fukuda, A Higashi, Y Matsuyama, C Nagoshi, J Nakano, M Sekimoto, P Tlusty, J Ahn, H En'yo, H Funahashi, Y Goto, M Iinuma, K Imai, Y Itow, S Makino, A Masaike, Y Matsuda, S Mihara, N Saito, R Susukita, S Yakkaichi, K Yoshida, M Yoshida, S Yamashita, R Takashima, F Takeutchi, S Aoki, M Iri, T Iijima, T Yoshida, I Nomura, T Motoba, Y Shin, S Weibe, M Chung, I Park, K Sim, K Chung, and J Lee. Cascade hypernuclei in the (K^-, K^+) reaction on ^{12}C. *Physical Review C - Brief Reports*, 1998.

[49] S Dairaku, H Fujimara, K Imai, S Kamigaito, K Miwa, A Sato, K Senzaka, K Tanida, C Yoon, R Chrien, Y Fu, C Li, X Li, J Zhou, S Zhou, L Zhu, K Nakazawa, T Watanabe, H Noumi, Y Sato, M Sekimoto, H Takahashi, T Takahashi, A Toyoda, E Evtoukhovitch, V Kalinnikov, N Karavchuk, A Moiseeneko, D Mzhavia, V Samoilov, Z Tsamalaidze, W Kallies, O Zaimdoroga, O Hashimoto, K Hosomi, T Koike, T Ma, M Mimori, K Shirotori, H Tamura, and M Ukai. Measurement of x rays from the Ξ^- atom. Technical report, J-PARC, 2006.

[50] J Carroll, A Thomas, J Rafelski, and G Miller. Nonperturbative relativistic calculation of the muonic hydrogen spectrum. *Physical Review A*, 2011.

[51] C Batty, E Friedman, and A Gal. Experiments with Ξ^- atoms. *Physical Review C*, 1999.

[52] S Takeuchiu, K Shimzu, and K Yazaki. Exchange currents arising from quark degrees of freedom. *Nuclear Physics A*, 1988.

[53] A Thomas. Chiral symmetry and the bag model. *Advances In Nuclear Physics*, 1984.

[54] R Barrett and D Jackson. *Nuclear sizes and structure*. Clarendon Press, Oxford, 1977.

[55] F Caruso, V Oguri, and F Silveira. Applications of the Numerov method to simple quantum systems using python. *Revista Brasileira de Ensino de Fisca*, 2022.